

# **Ubiquitination-deubiquitination by the TRIM27-USP7**

## **Complex Regulates TNF- $\alpha$ -induced Apoptosis**

(TRIM27-USP7 複合体によるユビキチン-脱ユビキチン化による TNF- $\alpha$  誘導性アポトーシス)

**2013**

筑波大学大学院博士課程人間総合科学研究科

**Mohammad Mahabub-Uz-Zaman**

筑波大学

博士（医学）学位論文

筑波大学

博士（医学）学位論文

Dedication

*This dissertation is dedicated to two ladies, my mother- Selina Akter and my wife- Tanya.  
Thank you for all your love, support, blessings and sacrifice throughout my life.*

## **Acknowledgement**

---

My doctoral thesis, while the culmination of several years of hard work, I feel represents only a fraction of what I have been fortunate to learn during my time as a higher degree research student. For this I must make special thanks to a number of people.

First and foremost, I offer my sincerest gratitude and respect to my supervisor, Professor Shunsuke Ishii for giving me the opportunity to work in his laboratory as a graduate student. He patiently provided the vision, encouragement and advice necessary for me to proceed through the doctoral program and complete my dissertation. His attention, knowledge, moral support and timely suggestions were always useful for my study. He was a role model for me. His attitude towards research inspired me and gives me the vision to be a member of the academic family.

I am also indebtly grateful to my mentor Dr. Teruaki Nomura for his valuable instruction, guidance and supervision throughout my experiments in this study. This thesis would not have been possible without his help and support.

My special thanks goes to my assistant advisor Dr. Toshie Shinagawa for her constant technical support and valuable advice about of my study. I am also grateful to Dr. Keisuke Yoshida and Dr. Toshio Maekawa for their countless support and help in several experiments. Also I would like to thank these people for sharing the lunch table very often with me and the discussions during the lunch time was a nice memory.

I would especially like to thank all my collaborators, Dr. Tsuyoshi Takagi, Dr. Tomoo Okamura, Dr. Wanzhu Jin and Dr. Yasunori Tanaka whose scientific expertise and support added important insights for my study.

I acknowledge and thank to our lab secretary Maruyama-San for her multifarious support during my stay at Riken, for keeping me away from all sorts of administrative work and making my life easy in Japan. I also wish to extend my thank to all other members of our laboratory for being always friendly with me. It has been a great privilege to spend several years in the laboratory of Molecular Genetics, RIKEN Tsukuba Institute and its members will always remain dear to me.

I must thank to RIKEN for providing me the financial support during my graduate study.

Finally, I would like to express my gratefulness and special thanks to my wife Tanya, my parents and other family members for believing on me, and for their patience, constant support and blessings throughout my study.

## 要約

TRIM27 (別名 RFP) は TRIM ファミリーに属し、RING ドメインを持つことから、ユビキチン E3 リガーゼと考えられてきた。いくつかの研究から、異なるユビキチン E3 リガーゼが様々な制御因子をユビキチン化することにより、アポトーシス、TNF- $\alpha$ 、自然免疫シグナリングに重要な役割を果たすことが示されている。しかし、TRIM27 のこれらのシグナリングにおける役割は不明である。また SNPs と疾患とのゲノムワイドリンクエージに関する研究から、ヒト TRIM27 遺伝子は、いくつかの自己免疫疾患に関与することが示唆されているが、実験的な証拠はない。本研究では、TRIM27 のアポトーシス、TNF- $\alpha$ シグナリングにおける役割を明らかにし、自己免疫疾患との関連を明らかにした。

マウスにTNF- $\alpha$ /GalN を投与すると、肝障害が誘導される。*Trim27*<sup>-/-</sup> 変異マウスでは、野生型マウスに比べ、肝障害の程度が明らかに弱かった。さらにマウス線維芽細胞では、TNF- $\alpha$  /CHX により誘導されるアポトーシスの程度が、野生型細胞に比べ低いことが示された。TNF- $\alpha$  シグナリングでは、complex I 依存性のsurvivalシグナリングとcomplex II 依存性のアポトーシスシグナリングの2つが存在する。前者の下流のNF $\kappa$ B 標的遺伝子 (*cFLIP*, *cIAP2*, *A20*, *ICAM*) の発現は、*Trim27*<sup>-/-</sup> 細胞と野生型細胞で差がなかった。一方、complex IIの形成を免疫共沈法で調べると、*Trim27*<sup>-/-</sup> 細胞ではcomplex II形成が低下していた。このメカニズムをさらに詳細に解析した所、1) TRIM27は脱ユビキチン化酵素USP7をユビキチン化し、その活性を活性化すること、2) 活性化されたUSP7はRIP1からユビキチンを除去することが示された。これまで他のグループにより、RIP1からの脱ユビキチンは、complex II 形成に必須であることが示されている。以上の結果から、TRIM27はUSP7を介して、RIP1の脱ユビキチン化を促進することにより、TNF- $\alpha$  によるアポトーシスを正に制御することが示された。

一方、TRIM27 と自己免疫疾患との関連を明らかにするため、streptozotocin (STZ) により誘導されるマウス糖尿病モデルを用いた。*Trim27*<sup>-/-</sup> マウスは野生型マウスに比べ、STZ 誘導性の糖尿病を発症し易いことが示された。*Trim27*<sup>-/-</sup> 細胞マウスでは、 $\beta$  細胞の減少、活性化 caspase-3 シグナルと T 細胞浸潤の亢進が認められた。以上の結果は、TRIM27 遺伝子の変異が、I型糖尿病などのある種の自己免疫疾患の発症に関与することを示唆するものである。

## **Abstract**

---

**Purpose:** TRIM27 (also known as the Ret Finger Protein, RFP) is one of the TRIM family proteins and due to the presence of RING domain in its structure, TRIM27 has been regarded as the ubiquitin E3 ligase enzyme for a long time. Several studies suggest that different E3 ligase enzymes play a key role in the regulation of apoptosis, TNF- $\alpha$  or innate immune signaling pathway by ubiquitinating various regulatory molecules. However, the role of TRIM27 in those pathways is still not clear. Although, previous study suggests that over-expression of TRIM27 in human embryonic kidney cell could induce the apoptosis but detailed mechanism is still unknown. Moreover, more than 30 genome-wide association studies, in several autoimmune diseases, identified hundreds of common variants, which suggested a linkage between *TRIM27* mutations and various autoimmune diseases but there is no experimental evidence in support of this hypothesis. In this context, the aim of our study is to unravel the mechanism of TRIM27 in apoptosis and TNF- $\alpha$  signaling pathway and find out its connection with autoimmune diseases by using murine model system.

**Materials and Methods:** *Trim27*<sup>-/-</sup> mice were generated by homologous recombination in TT2 ES cells. To understand the physiological role of TRIM27 in TNF- $\alpha$  induced apoptosis TNF- $\alpha$ /GalN-induced hepatitis mouse model were utilized. Mouse hepatitis were characterized by measuring serum ALT, AST, bioassay of caspase-3 and 8 in liver homogenate and histo-pathological analysis of liver tissue sections by TUNEL analysis, H&E staining and immunohistochemistry using cleaved caspase-3. Mouse embryonic fibroblasts (MEFs) were isolated from embryos at 14.5 days postcoitus and spontaneously immortalized MEFs were isolated. To examine cell viability of MEF, cells ( $1 \times 10^4$ ) were seeded into 96 well plates. At 24 h after incubation, cells were treated with various combination of recombinant mouse TNF $\alpha$ , cyclohexamide, anti-FAS antibody, TRAIL with enhancer antibody, etoposide or USP7 inhibitor HBX 41,108 for indicated time point and cell viability was assessed colorimetrically using the cell counting kit-8. Flow cytometry was used to check the expression of TNF- $\alpha$  receptor in MEF. NF $\kappa$ B activity was assessed by electrophoretic mobility shift assay. NF $\kappa$ B target gene expression was analyzed by Real-time RT-PCR. The subcellular localization of TRIM27, USP7 or RIP1 were performed immunohistochemically or biochemically by Nycodenz gradient fractionation. Protein levels of the apoptosis-regulating factors were

determined by Western blotting. Ubiquitination of endogenous and exogenously expressed proteins (RIP1, TRIM27 or USP7) were checked by *in vivo* ubiquitination assay in 293T and MEF cell line. Protein-protein interactions of TRIM27, USP7 and RIP1 or TNF- $\alpha$  induced complex II formation were checked by co-immunoprecipitation methods. shRNA and siRNA specific for USP7 were used for knockdown of USP7 in 293T or MEF cell line. Multiple low dose streptozotocin (STZ) induced diabetes model were used to assess the role of TRIM27 in autoimmune type I diabetes. Diabetes were characterized by measuring the blood glucose (by glucometer), insulin (by ELISA) and histopathological analysis of paraffin section of mouse pancreas by HE staining, anti CD3, anti-cleaved caspase-3 or anti-insulin immunohistochemistry.

**Results and Discussion:** As TRIM27 is an ubiquitin E3 ligase, and ubiquitination plays a role in the regulation of TNF- $\alpha$  signaling, we examined TNF- $\alpha$  signaling in *Trim27*<sup>-/-</sup> mice. We used a D-galactosamine (GalN) sensitized mouse model of liver injury in which TNF- $\alpha$  induces hepatocyte apoptosis in the presence of GalN. WT mice treated with TNF- $\alpha$  and GalN died within 10 h, whereas 60% of *Trim27*<sup>-/-</sup> mice treated under the same conditions survived and lived even 24 h after injection. TNF- $\alpha$ -induced apoptosis was further examined in primary MEFs. The viability of WT MEFs was significantly reduced when treated with TNF- $\alpha$  together with the protein synthesis inhibitor cyclohexamide (CHX). In contrast, TNF- $\alpha$  /CHX treatment only slightly reduced the cell viability of primary *Trim27*<sup>-/-</sup>.

To determine whether TRIM27 plays a role in TNF- $\alpha$  induced survival signaling, NF $\kappa$ B activity and NF- $\kappa$ B target gene expression of typical survival-related genes (including *cFLIP*, *cIAP2*, *A20*, and *ICAM* ) were assessed in the presence or absence of TNF- $\alpha$  . The result showed that NF $\kappa$ B activity and the expression levels of these genes were similar between WT and *Trim27*<sup>-/-</sup> MEF indicating that TRIM27 does not affect TNF- $\alpha$  survival signaling. To investigate the role of TRIM27 in the complex II-dependent apoptosis pathway, the complex II formation was compared between WT and *Trim27*<sup>-/-</sup> MEFs. The levels of RIP1 and caspase-8 co-immunoprecipitated with FADD were found lower in *Trim27*<sup>-/-</sup> cells than in WT cells after TNF- $\alpha$ /CHX treatment. These results suggest that TRIM27 is involved in the complex II-dependent apoptosis pathway, but not in the complex I-dependent survival signaling pathway.

As TRIM27 has been reported to have E3 ligase activity, we therefore hypothesized that the effect of TRIM27 on TNF- $\alpha$ -induced apoptosis may be mediated by ubiquitination of a regulatory factor. Of the several candidates examined, TRIM27 only affected the ubiquitination status of RIP1. However, contrary to its expected function as an Ub E3 ligase, TRIM27 deubiquitinated RIP1. In the co-immunoprecipitation assay, RIP1 was co-precipitated with TRIM27, suggesting the interaction between TRIM27 and RIP1. To understand the mechanism underlying the deubiquitination of RIP1 by TRIM27, TRIM27 interacting proteins were identified by purifying the complex formed. Through mass spectrometric analysis we determined the purified complex contained a 120-kD band identified as USP7 a ubiquitin-specific protease. USP7 colocalized with TRIM27 in the cytoplasm and in the nucleus of HepG2 cells and MEFs suggesting that these proteins interact. Furthermore, USP7 co-immunoprecipitated with TRIM27 cells transfected with the TRIM27 expression vector. To examine whether USP7 is needed for the TRIM27-induced deubiquitination of RIP1, we generated *Usp7*-knockdown 293T cell lines. When RIP1 was co-expressed with increasing amounts of TRIM27 in this cell line, RIP1 deubiquitination was not observed indicating that USP7 is required for the TRIM27-induced deubiquitination of RIP1. These results suggest that the TRIM27-USP7 complex binds to RIP1, resulting in its deubiquitination. To examine the role of TRIM27 in the TRIM27/USP7 complex-induced deubiquitination of RIP1, we investigated whether TRIM27 ubiquitinates USP7. Ubiquitination assays in 293T cells showed that TRIM27 mediates the addition of poly-Ub chains to USP7. Expression back of siRNA-resistant WT *USP7* mRNA in *Usp7*-knockdown 293T cells recovered the TRIM27-induced RIP1 deubiquitination, whereas overexpression of siRNA-resistant ubiquitin site mutant USP7-K869R mRNA did not. These results indicate that the ubiquitination of USP7 by TRIM27 is required for the TRIM27-induced deubiquitination of RIP1.

To confirm that USP7 plays a role in TNF- $\alpha$ -induced apoptosis, *Usp7* mRNA was down-regulated in immortalized MEF by using mouse siRNA. Down-regulation of USP7 made the cells resistant to TNF- $\alpha$ /CHX-induced apoptosis compared to control cells. We next examined the ubiquitination of endogenous RIP1 in response to TNF- $\alpha$ /CHX treatment using WT, *Trim27*<sup>-/-</sup>, and *Usp7* knockdown MEF cell lines. The level of ubiquitinated RIP1 in *Trim27*<sup>-/-</sup> cells and *Usp7* knockdown cells was higher than

in WT and control cells which further support that the TRIM27/USP7 complex plays a role in TNF- $\alpha$ -induced apoptosis by mediating RIP1 deubiquitination.

Multiple studies have suggested a link between TNF- $\alpha$  pathway and various diseases, such as diabetes. Here, we report that *Trim27*-deficient mice were susceptible to multiple low dose streptozotocin (STZ)-induced diabetes, a mouse model of diabetes. Infiltration of T cells and cleaved caspase-3 signals were enhanced, and  $\beta$ -cell mass was decreased in *Trim27*-deficient islets compared to wild-type islets. Our findings were also consistent with the results of recent genome-wide association studies linking autoimmune diseases and genetic polymorphisms, which showed an association between human TRIM27 genes and Type 1 diabetes. Although in this study we couldn't show any direct evidence in support of the mechanism of crosstalk between defective apoptosis and development of diabetes, however, as the *Trim27*<sup>-/-</sup> mice showed increased infiltration of lymphocyte in the pancreas in response to STZ, we speculate that peripheral lymphocyte homeostasis and self tolerance mechanism to minimize the accumulation of autoreactive lymphocytes might be defective in *Trim27*<sup>-/-</sup> mice due to abrogated TNF- $\alpha$ -induced apoptosis.

**Conclusion:** Here, we show that TRIM27, a tripartite motif (TRIM) protein containing RING finger, B-box, and coiled-coil domains, positively regulates TNF- $\alpha$ -induced apoptosis. *Trim27*-deficient mice are resistant to TNF- $\alpha$ /D-galactosamine-induced hepatocyte apoptosis. *Trim27*-deficient mouse embryonic fibroblasts (MEFs) are also resistant to TNF- $\alpha$ /cycloheximide-induced apoptosis. TRIM27 forms a complex with and ubiquitinates the ubiquitin-specific protease USP7, which deubiquitinates receptor-interacting protein 1 (RIP1), resulting in the positive regulation of TNF- $\alpha$ -induced apoptosis. *Trim27*-deficient mice were susceptible to streptozotocin (STZ)-induced diabetes, a mouse model of Type I diabetes. Our findings indicate that the ubiquitination-deubiquitination cascade mediated by the TRIM27-USP7 complex plays an important role in TNF- $\alpha$ -induced apoptosis.

## Table of Contents

---

Contents	Page No
<b>Acknowledgement</b>	i-ii
<b>Abstract (Japanese)</b>	iii
<b>Abstract (English)</b>	iv-vii
<b>Chapter 1: Introduction and Review of Literature.....</b>	1
1.1 Apoptosis.....	1
1.2 Ubiquitination-deubiquitination process and their role in apoptosis.....	4
1.3 TRIM Family Proteins.....	6
1.4 TRIM27.....	10
1.5 TNF- $\alpha$ signalling pathway.....	11
1.6 Balance between life and death.....	13
1.7 Connection of apoptosis, TNF receptor (TNFR) family and autoimmune disease..	13
<b>Chapter 2: Research Purpose and Objectives.....</b>	15
<b>Chapter 3: Materials and Methods.....</b>	16
3.1 Generation of <i>Trim-27</i> <sup>-/-</sup> mice.....	16
3.2 TNF- $\alpha$ /GalN-induced toxicity.....	16
3.3 Serum ALT and AST measurement.....	16
3.4 Assay of Caspase 3 and Caspase 8 activity.....	17
3.5 TUNEL assay.....	17
3.6 Histology and immunohistochemistry.....	17
3.7 Cell culture and cell viability assay.....	17
3.8 Electrophoretic mobility shift assay (EMSA).....	18
3.9 Flow cytometry.....	18
3.10 Real-time RT-PCR.....	18
3.11 Subcellular localization of TRIM27.....	19
3.12 Comparison of apoptosis-regulating factors by Western blotting.....	20
3.13 In vivo ubiquitination assay.....	20
3.14 Purification and characterization of the TRIM27 complex.....	22
3.15 Co-immunoprecipitation assays.....	22
3.16 Knockdown of USP.....	23

3.17 STZ-induced diabetes.....	23
3.17 Primers used in the study.....	24
<b>Chapter 4: Results.....</b>	<b>25</b>
4.1 TNF- $\alpha$ -induced apoptosis is impaired in <i>Trim27</i> -deficient mice.....	25
4.2 TRIM27 is not involved in TNF- $\alpha$ -induced survival signaling but required for TNF- $\alpha$ -induced apoptosis signaling.....	26
4.3 Localization of TRIM27 to mitochondria.....	28
4.4 TRIM27 induces RIP1 deubiquitination.....	29
4.5 USP7 is required for the TRIM27-induced deubiquitination of RIP1.....	30
4.6 Ubiquitination of USP7 by TRIM27 is required for the TRIM27-induced deubiquitination of RIP1.....	32
4.7 Deubiquitination of RIP1 by the TRIM27-USP7 complex is required for TNF- $\alpha$ -induced apoptosis.....	34
4.8 <i>Trim27</i> <sup>-/-</sup> mice are prone to STZ-induced diabetes.....	35
<b>Chapter 4: Discussion.....</b>	<b>60</b>
<b>Chapter 5: Conclusion.....</b>	<b>68</b>
<b>Chapter 6: References.....</b>	<b>69</b>

## List of Tables and Figures

---

<b>Table No.</b>	<b>Table Title</b>	<b>Page No.</b>
Table 3.1	Sequences of primers used	24
<b>Figure No.</b>	<b>Figure Title</b>	<b>Page No.</b>
Figure 1.1	Mechanism of Apoptosis	3
Figure 1.2	Ubiquitination and deubiquitination	5
Figure 1.3	General structure of the TRIM family proteins	7
Figure 1.4	TNF- $\alpha$ signaling pathway	12
Figure 4.1	Generation of <i>Trim27</i> -deficient ( <i>Trim27</i> <sup>-/-</sup> ) mice.	37
Figure 4.2	TNF- $\alpha$ induced apoptosis is impaired in <i>Trim27</i> deficient mice	38
Figure 4.3	<i>Trim27</i> <sup>-/-</sup> MEFs are resistant to TNF $\alpha$ induced apoptosis	39
Figure 4.4	TRIM27 is not involved in TNF- $\alpha$ -induced survival signaling	40
Figure 4.5	Effect of TNF- $\alpha$ treatment on <i>Trim27</i> and <i>Usp7</i> expression	41
Figure 4.6	TRIM27 is involved in the TNF- $\alpha$ -induced complex II formation	42
Figure 4.7	FAS-, TRAIL-, or etoposide-induced apoptosis	43
Figure 4.8	Subcellular localization of TRIM27	44
Figure 4.9	Localization of TRIM27 is not affected by TNF $\alpha$ in MEF	45
Figure 4.10	Biochemical proof for mitochondrial localization of TRIM27	46
Figure 4.11	TRIM27 deubiquitinates RIP1	47
Figure 4.12	TRIM27 forms a complex with USP7	48
Figure 4.13	USP7 is required for the TRIM27-induced deubiquitination of RIP1	49
Figure 4.14	TRIM27, RIP1 and USP7 forms a complex	50
Figure 4.15	TRIM27 ubiquitinate the USP7	51
Figure 4.16	TRIM27 induces RIP1 deubiquitination by ubiquitinating and activating USP7.	52

Figure 4.17	Effect of USP7 on TRIM27 ubiquitination	53
Figure 4.18	Autoubiquitination of TRIM27	54
Figure 4.19	USP7 is required for TNF- $\alpha$ induced apoptosis	55
Figure 4.20	TRIM27-USP7 regulation of RIP1 ubiquitination in the presence of TNF $\alpha$ and CHX.	56
Figure 4.21	<i>Trim27</i> <sup>-/-</sup> mice are prone to STZ-induced diabetes	57
Figure 4.22	Reduced $\beta$ -cell mass and increased apoptosis in STZ induced diabetic <i>Trim27</i> <sup>-/-</sup> mice.	58
Figure 4.23	STZ induced diabetic <i>Trim27</i> <sup>-/-</sup> mice showed severe infiltration of lymphocytes in pancreatic islet	59
Figure 5.1	Model describing the role of TRIM27-USP7 in TNF- $\alpha$ -induced apoptosis	67

## **Chapter 1**

### **1. Introduction and Review of Literature**

---

#### **1.1 Apoptosis**

Apoptosis is a tightly regulated cellular suicide process essential for normal development and tissue homeostasis of all multicellular organisms [1]. In addition, apoptosis is also used as a defense strategy against persistent viral infection, autoimmunity and the emergence of cancer [2]. Dysregulation of this exact program not only interferes with normal physiology but also often leads to pathology and disease. In particular, every immunological and oncological disease can be traced to defects in apoptosis, thus generating a great interest and urgency in the understanding of mechanisms that underlie apoptosis signaling.

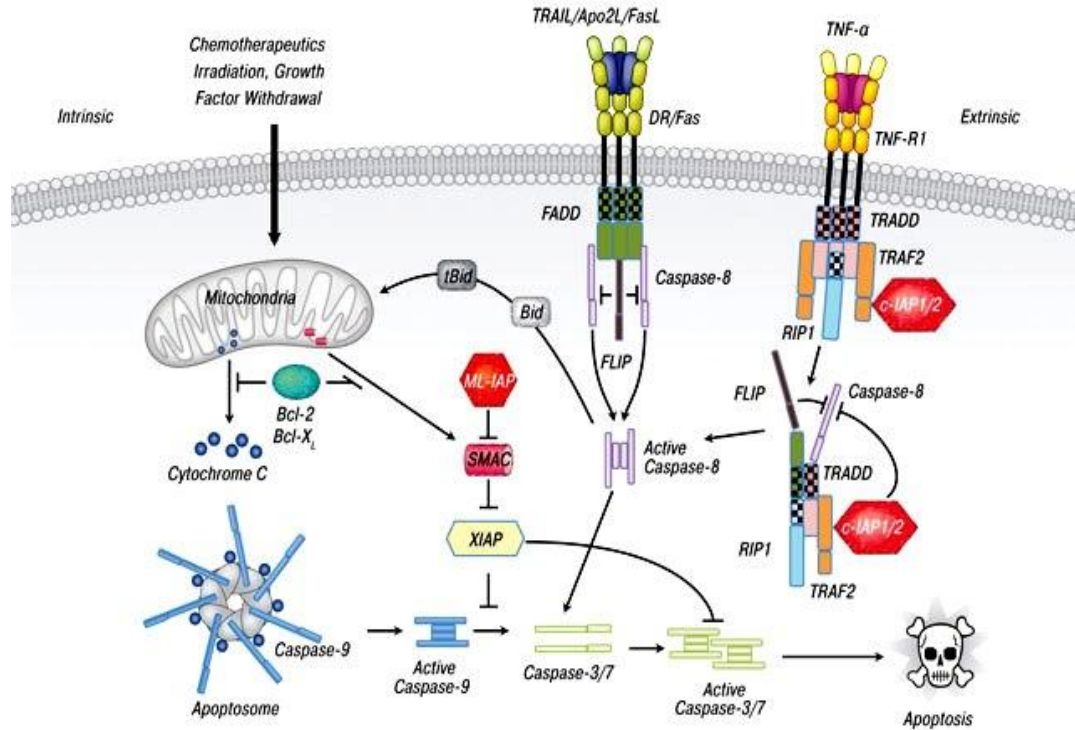
The name apoptosis originates from a Greek term meaning “the falling off of the leaves” [3]. The typical morphological features of apoptosis include- nuclear fragmentation, blebbing of the plasma membrane, cytoplasmatic shrinkage resulting in the formation of apoptotic bodies. Additionally, typical biochemical features of apoptosis are internucleosomal DNA fragmentation and externalization of molecules, such as phosphatidylserine, that are involved in the clearance of dead cells, allowing to recognize these cells and remove them [4-6].

The molecular apoptotic machinery in mammals is very complex and involves many redundant molecules (**Figure 1.1**). Diverse stimuli can trigger apoptosis, generally by affecting particular receptors (death receptors) or in a receptor-independent way by mitochondria or endoplasmic reticulum alteration [7].

The apoptotic cell death programme culminates in the activation of caspases, a family of highly specific cysteine proteases essential for the destruction of the cell [8]. Usually, caspases are expressed as inactive zymogens that are activated in cascades of auto- and trans-stimulation. Once activated, initiator caspases cleave and activate downstream effector caspases, thereby amplifying the proteolytic activity. Two major caspase-activating pathways have been identified [9]. Developmental cues or cellular stress such as DNA damage or Ca<sup>2+</sup> overload induce the 'intrinsic' pathway, whereas immune-mediated death-receptor stimulation activates the 'extrinsic' pathway. In the intrinsic pathway, both the permeabilization of the mitochondrial membrane and the release of pro-apoptotic molecules from the intermembrane space into the cytoplasm are crucial for activation of the initiator caspase caspase-9 [10]. Release of cytochrome c causes the formation of the apoptosome, a multicomponent adaptor complex that serves as a catalyst for caspase-9 oligomerization and activation [11].

By contrast, the extrinsic pathway is triggered through binding of an apoptotic signal (Fas, tumour necrosis factor - TNF) to a TNFR (TNF receptor) family protein (Fas/CD95/Apo-1, TRAIL, DR4, DR5 etc.) that initiate the assembly of caspase-8-activating platforms at the plasma membrane (**Figure 1.1**) [12]. Though the initiation and the spectrum of early caspase activation differ between intrinsic and extrinsic pathways, both pathways converge at the activation of caspase-4. In particular, caspase-3 functions as the most prevalent effector caspase. For example, DNA fragmentation mediated by caspase-activated DNase [CAD/DNA fragmentation factor-40 (DFF-40)] requires the caspase-3-mediated cleavage of its inhibitor of caspase

activated DNase (ICAD)/DFP-45 for nuclear translocation and activity [13].



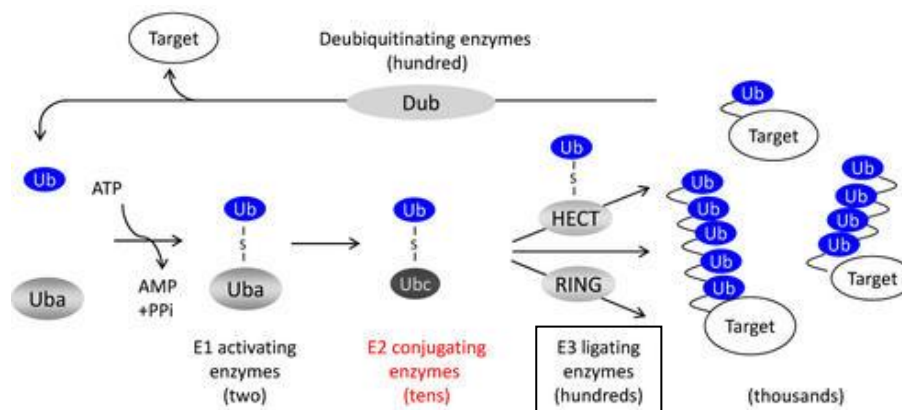
[Photograph source: Reference no. 12]

**Figure 1.1 Mechanism of Apoptosis.** Cell death in mammals is triggered by either extrinsic or intrinsic apoptotic molecular pathway. The extrinsic (receptor mediated) pathway includes binding of death ligands (FasL) to their receptors and subsequent requirement of adaptor molecules (FADD), thus forming a death inducing complex (DISC) within caspase-8 or -10 are cleaved into its active forms. Active initiation caspases promote apoptosis either by cleavage of a key execution caspase, caspase-3, or by Bid cleavage and mitochondrial apoptosis stimulation. The intrinsic (receptor independent) pathway of apoptosis is regulated mainly by Bcl-2 family proteins that control mitochondrial membrane permeability. Antiapoptotic Bcl-2 family proteins inhibit mitochondrial membrane pores opening, whereas proapoptotic Bcl-2 family (Bid, Bax, Bak) proteins induce the release of cytochrome c and other mitochondrial proteins from the intermembrane space into the cytoplasm. Cytochrome c subsequently binds Apaf-1 and caspase-9, activated initiation caspase-9 then cleaves caspase-4. Caspase-3 itself or other execution caspases (caspase-6, -7) cleave several proteins necessary for the cell survival causing cytoskeleton break-up, DNA fragmentation and cell death.

## 1.2 Ubiquitination-deubiquitination process and their role in apoptosis

Ubiquitination is a posttranslational modification that involves the covalent attachment of ubiquitin molecules to targeted proteins that are directed towards the ubiquitin proteasome pathway (UPP). UPP is the major system responsible for elimination of intracellular proteins especially misfolded cellular proteins in eukaryotes [14, 15]. This process regulates a number of cellular processes such as stability, function and localization of the targeted proteins. Ubiquitin, a 76 amino acid peptide, covalently attaches its C-terminal glycine to the  $\epsilon$ -amino group of substrate lysine residues in an isopeptide bond and is catalyzed by the sequential action of three enzymes, a ubiquitin-activating enzyme (E1), a ubiquitin-conjugating enzyme (E2), and a ubiquitin ligase (E3) (**Figure 1.2**) [15]. E1 activates ubiquitin through the formation of ATP-dependent thiol ester bond between the C terminus of ubiquitin and the active cysteine site of the E1, which is then transferred to active cysteine site of E3. Finally, E3 ligase catalyzes the transfer of ubiquitin to a lysine residue on the targeted protein (**Figure 1.2**). These ubiquitin chains can assemble in several different ways depending on the lysine site used to form the polyubiquitin chains including lysine K6, K11, K29, K48 and K63 [16]. It has been reported that ubiquitin chains can be formed from all these lysine residues on the substrate with various lengths and shapes in vitro and in vivo [17, 18]. Among them, polyubiquitin chains formed through K48 and K63 appear to be more frequent and have been extensively studied [17, 19]. K48-branched polyubiquitination is known to regulate protein stability and signals for proteasomal degradation of the substrate [15, 17]. Recently, K29 and K33-branched mixed chains

have been implicated in the regulation of AMP-activated protein kinase-related kinases [20]. Additionally, K29-branched ubiquitin chains promote the proteasomal and lysosomal degradation of proteins [21-23], whereas K63-branched polyubiquitination plays a key role in the regulation of endocytosis, DNA repair, protein kinase activation [24,25], signal transduction [26], intracellular trafficking of membrane proteins [26], and stress responses [27]. Taken together, UPP plays a major role in balancing the levels of critical proteins involved in major cellular processes such as cell cycle progression, DNA replication and repair, transcription, immune responses, and apoptosis [28-30].



[Photograph source: <http://www3.ie-freiburg.mpg.de/research-groups/epigenetics/pichler/regulation-of-ubiquitination-by-the-e2-enzyme-e2-25k/>]

**Figure 1.2 Ubiquitination and deubiquitination.** The process of ubiquitination is regulated by organized milieu of E1, E2 and E3 enzymes, which mediate the ligation of ubiquitin to the lysine residues in proteins. Ubiquitins can be recycled by the action of DUB enzymes.

Deubiquitination is a process where ubiquitinated proteins can be reversed to counterbalance the ubiquitination process by cleaving ubiquitin from ubiquitin-conjugated protein substrates with the help of DUBs (**Figure 1.2**) [27–29]. To

date, nearly 100 DUBs have been identified from the human genome and have been divided into at least five major families: UBP or USP (ubiquitin-specific processing proteases), UCH (ubiquitin carboxy terminal hydrolases), JAMM (Jad1/Pad/MPNdomain- containing metallo enzymes), OTU (Otu-domain ubiquitin–aldehyde-binding proteins) and Ataxin-3/Josephin [29].

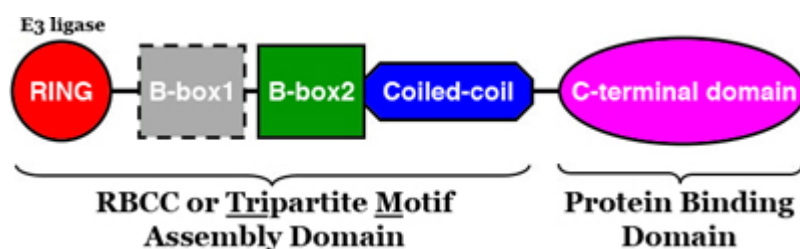
The entry of ubiquitin into the apoptosis arena began approximately one decade ago, with reports correlating increases in ubiquitin expression during programmed cell death in the intersegmental muscle (ISM) of insects and mature lymphocytes. Today, it is clear that ubiquitin is critically involved in the regulation of molecules at every phase of apoptosis and has opened an interesting new frontier in the study of apoptosis signaling [31-35].

There is a growing recognition that deubiquitination are also involved in the process of switching from prosurvival signaling to cell death signaling. These DUBs either up- or down-regulate their protein level or actively regulate their substrates when a cell encounters stressors such as DNA damage, unfolded protein, and oxidative stress signaling eventually resulting in cell death [36]. Recent studies on the role of DUBs have proven productive in revealing its role in the process of apoptosis.

### **1.3 TRIM Family Proteins**

The tripartite motif (TRIM) family of proteins is defined by a set of domains known as the RBCC motif, which consists of the RING (really interesting new gene 1) finger, one or two B-box motifs, and a coiled-coil region (**Figure 1.3**) [37]. The RING finger is a zinc-binding domain with an important role in ubiquitin (Ub) E3 ligase binding to

Ub-conjugating enzymes (E2) [38]. B-box is structurally related to the RING domain and are required for various biological functions [39], although their roles remain unclear. The coiled-coil region is mainly involved in homo- and hetero-dimeric interactions for large complex formation [40].



[Photograph source: <http://kumerowgen677s13.weebly.com/motifs-and-domains1.html>]

**Figure 1.3 General structure of the TRIM family proteins.** TRIMs share a common domain organization, with an N-terminal RING domain, followed by a B-box 2 domain, a coiled-coil domain, and a C-terminal domain. (Some TRIMs contain a B-box 1 domain in between the RING and B-box 2 domains.) RING domains are known to function as E3 ligases, and facilitate covalent modification of targets with ubiquitin or ubiquitin-like proteins. TRIM C-terminal domains are variable in nature, but generally appear to mediate interactions with other protein partners.

**Ring domain:** The RING domain is defined by a regular arrangement of cysteine and histidine residues that coordinate two atoms of zinc [41]. The RING zinc ligation system, which is unique to this domain, produces a single integrated structure referred to as the ‘cross-brace’ motif. This peculiar structure is the result of zinc coordination mediated for the first atom by Cys in position 1,2,5,6 and for the second atom by Cys or His in position 3,4,7,8 [42, 43]. There are two main RING subtypes, H2 and C2 [44]. The C2 type, which is characterized by a Cys residue in the fifth coordination site, is

found in the TRIM/RBCC family. There are few family members that do not present a RING domain and are still considered TRIM/RBCC because the rest of the motif (B-boxes and coiled-coil) is conserved in order and spacing. With few exceptions, the RING domain is typically found within 10–20 amino acids of the TRIM/RBCC protein first methionine [45, 46]. Functionally, the RING finger domain has been found to play a critical role in mediating the transfer of ubiquitin both to heterologous substrates as well as to the RING proteins themselves. This domain is therefore a characteristic signature of many E3 ubiquitin ligases.

**B-box domain:** The B-box domain is another zinc-binding motif that occurs in two flavors, B-box1 and B-box2, which share a similar but distinct pattern of cysteine and histidine residues [46, 48]. They mainly diverge in the second potential coordination residue, which is a cysteine in B-box1 and a histidine in B-box3. When both B-box domains are present, type 1 always precedes type 2; when only one B-box domain is present it is always the type 2 [46]. Due to the similarities between these domains, it is possible that B-box1 also coordinates one atom of zinc. To date, no specific function has been attributed to the B-box domains.

**Coiled-coil domain:** A coiled-coil region invariably follows the B-box2 in the entire set of TRIM/RBCC proteins [46, 48]. This predicted region is approximately 100 residues long, and is frequently broken up into two or three separate coiled-coil motifs. The coiledcoil region in the TRIM/RBCC proteins is mainly involved in homo-interactions and in promoting the formation of high molecular weight complexes and the definition of discrete subcellular compartments within the cell [46].

**C-terminal domain of TRIM family proteins:** While the tripartite motif, and especially the B-box domain, is restricted to this protein family, the C-terminal domains found in the TRIM/RBCC family members are also present in otherwise unrelated proteins. The most-common C-terminal motifs in the TRIM/RBCC proteins are the B30.2 domain, the NHL repeats and the associated PHD-BROMO domain. Approximately two thirds of the TRIM/RBCC proteins possess a B30.2 domain also known as RFP-like domain having been first identified in TRIM27/RFP. This 170-residue domain of unknown function is also present in a growing number of non-TRIM/RBCC proteins. It is composed of three blocks named after the more-conserved amino acid stretches, LDP (also known as PRY domain), WEVE and LDYE (also known as SPRY domain) motifs [49]. A less-frequent C-terminal domain within the TRIM/RBCC family is the NHL domain. It consists of 2–6 repeats, usually 5 or 6 in the TRIM/RBCC proteins, of an approximately 40-residue sequence that resembles the WD repeat and that assembles to form a multiblade propeller structure [50]. No function has been unequivocally attributed to any of the above-mentioned C-terminal domains to postulate their role in TRIM/RBCC protein function.

**Functions of TRIM family proteins:** Many TRIM proteins are induced by interferons (IFNs), which are crucial for resistance to pathogens, and a series of recent studies indicates that some TRIM proteins play an important role in the broader immune response [51]. For instance, TRIM25 ubiquitinates the caspase recruitment domains (CARD) of RIG-I (retinoic acid inducible gene I), a cytosolic receptor for viral RNAs, and this ubiquitination is required for IFN $\beta$  production and NF- $\kappa$ B promoter activation

[52]. TRIM30 $\alpha$  negatively regulates Toll-like receptor (TLR)-mediated NF- $\kappa$ B activation by targeting the adaptors TAB2 [TGF $\beta$ -activated kinase 1 (TAK1)-binding protein 2] and TAB3 for degradation, which results in the inhibition of TRAF6 (TNF receptor-associated factor 6) activity and I $\kappa$ B $\alpha$  phosphorylation [53]. TRIM56 induces K63-linked polyubiquitination of STING (stimulator of interferon genes), which regulates intracellular DNA-mediated, type I IFN-dependent innate immunity [54]. This ubiquitination is required for STING dimerization, TBK1 (TANK (TRAF family member-associated NF- $\kappa$ B activator)-binding kinase 1) recruitment, and IFN $\beta$  promoter activation. TRIM23 mediates K27-linked ubiquitination of NEMO (NF- $\kappa$ B essential modulator), which is important for NF- $\kappa$ B activation downstream of RIG-like receptor and TLR3 in response to viral dsRNA [55].

#### **1.4 TRIM27**

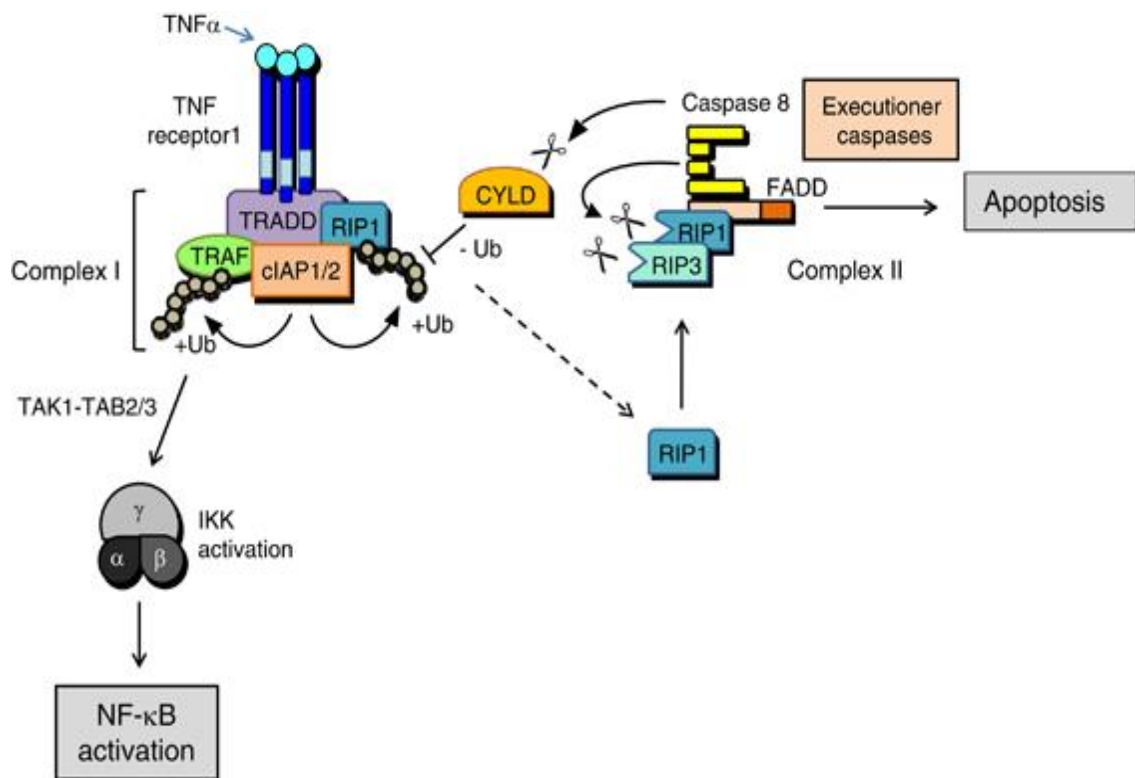
TRIM27 (also known as the Ret finger protein, RFP) is one of the TRIM family proteins, and was originally found to be fused to the *ret* proto-oncogene in transformed NIH3T3 cells [56]. TRIM27 plays a role in transcriptional regulation through interaction with Rb and the Mi-2 $\beta$ -containing histone deacetylase complex in the nucleus [57, 58]. TRIM27 contains a nuclear export sequence and shuttles between the cytoplasm and the nucleus [59]. In the cytosol, TRIM27 interacts with the IKK family of kinases and with TBK1, which inhibits NF- $\kappa$ B-dependent and IRF3-dependent transcriptional activation [60]. This inhibition does not depend on the RING finger of TRIM27, and the mechanism underlying the negative regulation by TRIM27 has not been elucidated. Previous study showed that RBCC moiety of TRIM27 triggers a rapid apoptosis through activation of

stress activated MAP kinases and caspases which indicate that RBCC moiety might participate in the control of cell survival. However, detailed mechanism was not elucidated [61]. Recent study suggests that TRIM27 inhibits the muscle differentiation by modulating serum response factor and enhancer polycomb1 in the nucleus [62]. TRIM 27 has also been shown to negatively regulate the CD4 T cells by ubiquitinating the class II PI3K-C2 $\beta$  in the K48 linked manner [63]. In another study TRIM 27 was reported to regulate the activation of IgE receptor of mast cells [64].

### **1.5 TNF- $\alpha$ signaling pathway**

TNF- $\alpha$  (tumor necrosis factor- $\alpha$ ) is a potent inflammatory cytokine that induces apoptosis of tumor cells but not normal cells, with the exception of hepatocytes, neural cells, and thymocytes [65]. Dysregulation of TNF- $\alpha$  signaling is often correlated with autoimmune diseases, including type 1 diabetes and Crohn's disease [66]. Recent studies have shown that ubiquitination plays a crucial role in TNF- $\alpha$  signaling [67]. Upon binding to TNF- $\alpha$ , TNFR1 (TNF receptor 1) recruits TRADD (TNFR1-associated death domain protein) [68] and triggers the formation of two distinct complexes: complex I and II [69] (**Figure 1.4**). The membrane-associated complex I, which activates NF- $\kappa$ B, contains TRADD, TRAF2, TRAF5, RIP1 (receptor-interacting protein kinase 1), cIAP1 (cellular inhibitor of apoptosis 1) and cIAP3. Both cIAP1 and cIAP2 are RING finger-containing ubiquitin ligases that catalyze the K-63-linked polyubiquitination of RIP1 [70, 71]. K-63 linked polyubiquitin chains recruit TAK1 and IKK complexes by binding to the regulatory subunits TAB2 and NEMO, activating NF- $\kappa$ B to induce a group of cell survival genes [72]. Activation of NF- $\kappa$ B via complex I

triggers the dissociation of TRADD, RIP1 and TRAF2 from complex I and the formation of cytoplasmic complex II, which contains FADD (Fas-associated death domain protein) and procaspase-8. Procaspase-8 is processed into the mature caspase-8, which cleaves procaspase-3 into the mature effector caspase-3 to initiate apoptosis [69].



[Photograph source: Reference no. 77]

**Figure 1.4 TNF- $\alpha$  signaling pathway.** In response to TNF- $\alpha$  stimulation, RIP1 is recruited to TNFR and forms a membrane associated complex I with TRADD, TRAF2/5 and cIAP1/2, which in turn leads to polyubiquitination of RIP1 and pro-survival NF- $\kappa$ B activation. RIP1 switches function to a regulator of cell death when RIP1 is deubiquitinated by A20 or CYLD. Deubiquitination of RIP1 leads to the formation of cytosolic DISC with FADD and caspase-8, the so-called complex II. Activation of caspase-8 in DISC leads to apoptosis induction.

## **1.6 Balance between life and death**

The balance between complex I-dependent cell survival and complex II-dependent apoptosis is regulated by multiple factors, and TNF- $\alpha$  does not induce apoptosis in most cells. NF- $\kappa$ B activation rapidly induces the expression of several anti-apoptotic proteins including cIAPs and c-FLIP (cellular FLICE-inhibitory protein), which prevent the activation of procaspase-8. NF- $\kappa$ B upregulates the expression of A20, which forms a ubiquitin-editing complex that removes K63-linked poly-Ub chains to induce RIP1 degradation [73, 74]. Another deubiquitinating enzyme, CYLD, which is the product of the cylindromatosis tumor suppressor gene *CYLD*, also specifically cleaves K63-linked poly-Ub chains bound to RIP1, releasing RIP1 from complex I and promoting the formation of complex II [75-76]. However, additional factors regulating the balance between TNF- $\alpha$ -induced apoptosis and cell survival may exist.

## **1.7 Connection of apoptosis, TNF receptor (TNFR) family and autoimmune disease**

There is accumulating evidence that apoptosis, programmed cell death, plays a pivotal role in the pathogenesis of autoimmune diseases [78]. A common feature of autoimmune diseases is the break down to tolerance of self antigens, a consequence of which is the production of auto-antibodies reactive with multiple self proteins. Apoptosis acts as a source of immunogens. It has been speculated that highly accelerated rates and/or abnormal sites or abnormal processing of apoptotic cells could lead to autoantibody production. Defects of apoptotic pathways in T cells promote the survival of potentially autoreactive, proinflammatory cells. Failure to eliminate activated cells can result in prolonged effector functions, such as CD40 ligand "help"

for B cells, inappropriate survival of primed autoantibody-producing B cells, or cytokine release by macrophages. Many organ specific autoimmune diseases are characterized by immune cell infiltrations that induce the apoptosis [78].

The mammalian immune system must balance the need for effective immune protection against pathogens with the requirement for tolerance to self-antigens to prevent autoimmune reactions [79, 80]. Immune tolerance is maintained through deletion of self-reactive lymphocytes (by cell death), functional inactivation (anergy), or suppression of cell activation via regulatory lymphocytes. Members of the tumor necrosis factor (TNF) and TNF receptor (TNFR) family play key roles in the development and function of the immune system. Altered regulation of several of these factors, such as TNF, TRAIL, CD40L and FasL, may contribute to a breakdown in immune tolerance and the development of various autoimmune disease like diabetes, experimental autoimmune encephalomyelitis (EAE), inflammatory bowel disease (IBD), multiple sclerosis (MS), rheumatoid arthritis (RA), systemic lupus erythematosus (SLE) etc. [66, 79, 80].

## Chapter 2

### **2. Research Purpose and Objectives**

---

TRIM27 (also known as the Ret finger protein, RFP) is one of the TRIM family proteins and due to the presence of RING domain in its structure, TRIM27 has been regarded as the ubiquitin E3 ligase enzyme for a long time. Several studies suggest that different E3 ligase enzymes play a key role in the regulation of various important biological signaling pathways including innate immune signaling, TNF- $\alpha$  signaling or apoptosis by ubiquitination [51, 67]. TRIM27 has been reported to contain a nuclear export sequence and shuttle between nucleus and cytoplasm [59] and shown to regulate the innate immune signaling pathway [60], muscle differentiation [62], and the activity of CD4 T cells and mast cells [63, 64] through its ubiquitin E3 ligase activity but its role in the apoptosis and TNF- $\alpha$  signaling pathway was not elucidated. Although a previous study suggests that overexpression of TRIM27 in human embryonic kidney cell could induce apoptosis [61], but detailed mechanism is still unknown. Moreover, more than 30 genome-wide association studies, in several autoimmune diseases, identified hundreds of common variants, which suggested a linkage between *TRIM27* mutations and various autoimmune diseases [82, 83] but there was no experimental evidence in support of this hypothesis. In this context, the aim of our study was to unravel the mechanism of TRIM27 in apoptosis and TNF- $\alpha$  signaling pathway and find out its connection with autoimmune diseases by using murine model system.

## Chapter 3

### 3. Materials and Methods

---

#### 3.1 Generation of *Trim-27*<sup>-/-</sup> mice

*Trim27*<sup>-/-</sup> mice were generated by homologous recombination in TT2 ES cells as described previously [84]. The *Trim27* gene was disrupted by replacing the 560-bp DNA fragment, which corresponds to the 430 bp upstream from the ATG initiation codon and the 130 bp of exon 1, with a neomycin cassette (**Figure 4.1**). This resulted in the deletion of the N-terminal initiator codon and the RING finger. *Trim27*<sup>-/-</sup> C57BL/6 congenic mice were generated by backcrossing onto a C57BL/6 genetic background for more than ten generations. All mice used were 8-10 week-old males. Experiments were conducted in accordance with the guidelines of the Animal Care and Use Committee of the RIKEN Institute.

#### 3.2 TNF- $\alpha$ /GalN-induced toxicity

Mice were sensitized by intraperitoneal administration of GalN [d-(+)-galactosamine hydrochloride, Sigma] at 700 mg per kg body weight. After 15 min of GalN treatment, recombinant mouse TNF- $\alpha$  (20  $\mu$ g/kg, Peprotech) was administered intraperitoneally and the mortality rate was measured over the next 24 h.

#### 3.3 Serum ALT and AST measurement

Blood was collected from the saphenous vein at 4 h after TNF- $\alpha$ /GalN treatment, serum was prepared and ALT, AST activities were analyzed by colorimetric method according to manufactures protocol (BioVision).

### **3.4 Assay of Caspase 3 and Caspase 8 activity**

Caspase-3/8 activities were measured using caspase3/8 colorimetric activity assay kit (Millipore). At 6h after TNF-a/GalN treatment, liver was collected and homogenized in a Dounce homogenizer by extraction buffer (Millipore). After brief centrifugation, caspase-3/8 activities of the homogenate were measured according to the manufacture's protocol (Millipore).

### **3.5 TUNEL assay**

To examine apoptosis in hepatic cells, mouse livers were excised 6 h after treatment and fixed in 4% paraformaldehyde. Paraffin-embedded sections (5  $\mu\text{m}$ ) were analyzed by TUNEL assay using an In Situ Cell Death Detection kit (Roche).

### **3.6 Histology and immunohistochemistry**

Histopathological analysis of paraffin embedded liver tissue sections were performed by H&E staining. Cleaved caspase-3 immunohistochemistry was performed as described by Bellenger *et al.* [85] using anti-cleaved caspase-3 antibody (Cell Signaling Technology).

### **3.7 Cell culture and cell viability assay**

Mouse embryonic fibroblasts (MEFs) were isolated from embryos at 14.5 days postcoitus. Spontaneously immortalized MEFs were isolated. MEFs, the human hepatoma cell line HepG2, and the human embryonic kidney cell line 293T were cultured in Dulbecco's modified Eagle's medium (Nissui Pharmaceuticals) with 10% bovine calf serum (HyClone) or fetal calf serum (Roche). To examine cell viability of MEF, cells ( $1 \times 10^4$ ) were seeded into 96 well plates. At 24 h after incubation, cells were

treated with various combination of recombinant mouse TNF $\alpha$  (PeproTech), cyclohexamide (Sigma), anti-FAS antibody (BD Bioscience), TRAIL with enhancer antibody (Enzo life science), Etoposide (Sigma) or USP7 inhibitor HBX 41,108 (Calbiochem) for indicated time point as described in the figure legends and cell viability was assessed colorimetrically using the cell counting kit-8 (Dojindo, Tokyo).

### **3.8 Electrophoretic mobility shift assay (EMSA)**

MEFs ( $1 \times 10^6$ ) were cultured for 24 h, and treated with TNF- $\alpha$  (20 ng/ml) for indicated time points as described in the figure legend. Nuclear extracts were prepared and subjected to EMSA using  $^{32}\text{P}$ -radiolabelled double-stranded NF- $\kappa\text{B}$  probe (AGTTGAGGGGACTTTCCCAGGC) as described by Thapa et al. [86]. For super shift assay, nuclear extract was pre-incubated with anti-p65 antibody (Santa Cruz) on ice for 10 min before addition of radiolabelled NF- $\kappa\text{B}$  probe.

### **3.9 Flow cytometry**

One day after culture, MEF cells were collected with trypsin, washed with PBS and FACS buffer (1% BSA/PBS) and blocked using Fc block reagent (BD Bioscience) and stained with PE conjugated anti-mouse TNFR antibody (Biolegend) for 30 min at 4°C. Cells were washed twice with FACS buffer and analyzed by FACSCalibur flow cytometer (Becton Dickinson).

### **3.10 Real-time RT-PCR**

Total RNA was isolated from MEFs using Trizol (Invitrogen). Real-time reverse transcription-PCR (RT-PCR) was performed using an ABI 7500 Real-Time PCR Instrument and the QuantiTect SYBR Green one step RT-PCR kit (Qiagen), according

to the manufacturer's instructions. The PCR conditions were 50°C for 30 min, 95°C for 15 min, and 40 cycles of 94°C for 15 s, 60°C for 35 s and 72°C for 35 s. The primer sequences are shown in **Table 3.1**. The relative level of mRNA expression was normalized against the amount of 18S rRNA using rRNA Control Reagents (Applied Biosystems).

### **3.11 Subcellular localization of TRIM27**

The subcellular localization of TRIM27 and USP7 was immunohistochemically examined as described previously (59). HepG2 cells or MEFs were transfected with 3 or 1.5 µg of the expression vector using Lipofectamine (Invitrogen). Forty-eight hours after transfection, cells were fixed and stained with anti-FLAG antibody M2 (Sigma) and MitoTracker Red CMXRos (Molecular Probes) or rabbit polyclonal anti-USP7 antibody (Bethyl Laboratories). The signals were visualized by rhodamine- or fluorescein isothiocyanate-conjugated secondary antibodies (Jackson ImmunoResearch), and analyzed by confocal microscopy (Zeiss LSM510). For Nycodenz gradient fractionation, immortalized MEF cells were transfected with the FLAG-TRIM27 or FLAG-RIP1 expression plasmid, harvested in ice-cold homogenizing buffer (10 mM Tris-HCl, pH 7.4, 250 mM sucrose, 5 mM EDTA, and protease inhibitor mixture), and passed 50 times through a Potter-Teflon homogenizer on ice. A post-nuclear supernatant was obtained (3,000 rpm, 10 min, 4°C) and subjected to Nycodenz gradient fractionation as described previously [87].

### **3.12 Comparison of apoptosis-regulating factors by Western blotting**

MEFs were lysed by mild sonication in SDS sample buffer and boiled for 5 min. Protein concentration was determined by Lowry method (BioRad Laboratories) and 25-50  $\mu$ g protein was typically subjected to SDS-PAGE. Anti-cleaved caspase-3 (Cell Signaling), anti-TNFR1 (R&D Systems), anti-TRADD (Santa Cruz), anti-TRAF2 (Santa Cruz), anti-RIP1 (BD Bioscience), anti-FADD (Santa Cruz), anti-CYLD (Santa Cruz), anti-USP7 (Bethyl laboratories), anti-TRIM27 (IBL Chemicals), and anti- $\alpha$ -tubulin (Sigma) antibodies were utilized to check the respective endogenous protein levels by Western blotting.

### **3.13 *In vivo* ubiquitination assay**

For ubiquitination assay of exogenously expressed proteins, HEK293T or HepG2 cells were transfected with a mixture of the indicated plasmids and empty vector using the calcium phosphate precipitation method. The plasmids used are pact-FLAG-RIP1, pact-FLAG-USP7, pact-3xMyc-Ub to express various forms of Ub, pact-TRIM27 to express various forms of TRIM27, including FLAG-tagged or His-tagged TRIM27, RING finger mutant, in which Cys-16, Cys-19, Cys-31, and His-33 were replaced with Ala, B-box mutant, in which Cys-96, Cys-99, His-107, and Asp-110 were replaced by Ala, 4KR mutant in which Lys-79, Lys-304, Lys-380, Lys-382 were replaced with Arg. For immunoprecipitation of Flag tagged proteins, at 40 h post-transfection, the cells were lysed in 1% SDS-containing RIPA buffer by sonication. Lysates were then precleared and diluted with buffer lacking SDS to reduce the SDS concentration to 0.1%, and immunoprecipitated overnight at 4°C with anti-FLAG M2 monoclonal

antibody (Sigma). Immunocomplexes were captured with protein G sepharose beads (GE healthcare), washed three times with NETN buffer containing 1 M NaCl and 2% NP40, eluted with SDS sample buffer by boiling, and then separated by 7% SDS-PAGE and analyzed by immunoblotting. In the case of His-tagged TRIM27, transfected cells were scraped into urea buffer (8 M urea, 0.1 M sodium phosphate, pH 8.0, 0.3 M NaCl, 10 mM *N*-ethylmaleimide), and sonicated mildly on ice, and His-TRIM27 was purified using a HIS-select cobalt affinity gel (Sigma). Western blotting was performed as described above.

In case of endogenous ubiquitination assay, cells were stimulated with mouse TNF- $\alpha$  (10 ng/mL) and cycloheximide (1  $\mu$ g/mL), and lysed with 1% SDS-containing RIPA buffer supplemented with 10 mM *N*-ethylmaleimide and protease inhibitors by vortexing and boiling for 5 min. Lysates were sonicated mildly on ice, diluted and precleared with sepharose beads for 1 h at 4°C on a rotating wheel, and immunoprecipitated overnight at 4°C with anti-RIP-1 antibody (BD Biosciences) or anti-USP7 antibody (Bethyl laboratories). Immunocomplex was captured, washed, eluted and resolved as described above. Following transfer of proteins to nitrocellulose membrane, the membrane was autoclaved before incubation at denaturing buffer (6 M guanidine-HCl, 20 mM Tris-HCl pH 7.5, 5 mM  $\beta$ -mercaptoethanol, 1 mM PMSF) for 30 min at 4°C. After extensive PBS washing, membrane was blocked at 20% heat inactivated bovine calf serum and immunoblotting was performed with anti-Ub (Invitrogen) or anti-K63-linked Ub (Millipore) antibody using immunoreaction enhancer solution (Toyobo).

### **3.14 Purification and characterization of the TRIM27 complex**

Purification of the complex was performed as described previously [88]. The HeLa S3 cell clone expressing FLAG/HA-TRIM27 was generated. Cells from a 4 L culture were disrupted in hypotonic buffer, and the nuclear pellet was collected by centrifugation at 25,000 g for 20 min. The pellet was extracted with buffer C (20 mM HEPES, pH 7.9, 25% glycerol, 420 mM NaCl, 1.5 mM MgCl<sub>2</sub>, 0.2 mM EDTA, 0.5 mM PMSF, and 0.5 mM DTT) and lysates were collected by centrifugation. The TRIM27 complex was purified using anti-FLAG M2 monoclonal antibody (mAb)-conjugated agarose beads followed by anti-HA 12CA5 mAb-conjugated agarose beads in wash buffer. The purified proteins were separated by 4–20% gradient SDS-PAGE and silver stained. The protein bands were excised and analyzed by mass spectrometry. Anti-TRIM27 (IBL-America) or anti-USP7 (Bethyl Laboratories) antibody was used for immunoblotting.

### **3.15 Co-immunoprecipitation assays**

For co-immunoprecipitation experiments, 293T cells were directly used or transfected using the CaPO<sub>4</sub> method with various plasmid mixtures, as described in the figure legends. Cells were collected and lysed by mild sonication in NETN buffer (20 mM Tris-HCl pH 8.0, 150 mM NaCl, 1% NP-40, 1mM EDTA, 10% glycerol and protease inhibitor cocktail). Lysates were then diluted, pre-cleared and subjected to immunoprecipitation by incubation with indicated antibodies for overnight at 4°C. The immunocomplexes were captured by protein G sepharose beads, washed three times with the lysis buffer containing 0.2% NP-40 and separated by SDS-PAGE. Western

blotting was performed using the antibodies described in the figure legends and the ECL Western blotting System (Millipore). Aliquots of the lysates were also analyzed by Western blotting. For TNF- $\alpha$  induced complex II analysis, MEFs were treated with TNF- $\alpha$  (100 ng/ml) and Cyclohexamide (1  $\mu$ g/ml) for the indicated time period as described in the figure legend and FADD/Caspase8/RIP1 complex was isolated and analyzed as reported by Ramakrishnan and Baltimore [89].

### **3.16 Knockdown of USP**

The previously reported sequence of shRNA against human USP7 [90] was cloned into the pSuper.puro vector and transfected into 293T cells, which were selected with 1  $\mu$ g/mL of puromycin (Sigma). Cell lysates from the isolated clones were used for Western blotting to examine the levels of USP7. For MEFs, the *Usp7* gene was knocked down using siRNA specific for mouse USP7 (Invitrogen, target sequence: 5'-GACCCUGGAUUUGUGGUCACAUAU-3'). For gene-specific knockdown, immortalized MEFs were plated in 6 well plates and transfected with 10  $\mu$ M control or USP7-specific siRNA using Lipofectamine RNAiMAX (Invitrogen). Forty-eight hours after transfection, cell lysates were prepared and USP7 was detected by Western blotting.

### **3.17 STZ-induced diabetes**

For the STZ-induced diabetes model, male mice aged 8 weeks were injected intraperitoneally for five consecutive days with STZ (Sigma) dissolved in citrate buffer (pH 4.5) at a concentration of 40 mg/kg. Blood glucose level was measured weekly in non-fasted animals from the tail vein using a glucometer (Sanwa Kagaku Kenkyusho

Co., Ltd., Japan). Sixty days after the first injection, mice were sacrificed, and the whole pancreas was collected, fixed in 4% paraformaldehyde and embedded in paraffin. Sections were prepared from three parts of the pancreas and stained with hematoxylin and eosin to determine the degree of lymphocyte infiltration. Tissue sections were also analyzed by immunohistochemistry with an anti-insulin antibody (C27C9, Cell Signaling Technology), anti-cleaved caspase-3 (cell signaling) and anti-CD3 antibody (Abcam) as described previously [85]. For serum insulin measurement, non-fasting blood was collected from the saphenous vein of mice before killing. Serum was snap frozen in liquid nitrogen and stored at -80°C until determination of insulin concentration with a mouse ELISA kit (Merckodia).

### 3.18 Primers used in the study

Primers used for qRT-PCR and for genotyping of mouse are shown in Table 3.

**Table 3.1 Sequences of primers used.**

qRT-PCR		
<i>Gene</i>	Forward (5'→3')	Reverse (5'→3')
<i>A20</i>	GAACAGCGATCAGGCCAGG	GGACAGTTGGGTGTCTCACATT
<i>cFLIP</i>	GACTCTAAGCCCCTGCAACC	GGAGGGCTTCTCCAAGTGAG
<i>cIAP2</i>	ACGCAGCAATCGTGCATTTTG	CCTATAACGAGGTCCTGACGG
<i>ICAM</i>	CAGATCCTGGAGACGCAGAG	GAACCACCTTCGACCCACTG
<i>Usp7</i>	GCGTGGGACTCAAAGAAGC	GAATCATCGCCCTCTGTTGG
<i>Trim27</i>	CTTCGTGGAGCCTATGATGC	CTGCGGACACGACACGTTAG
Mouse genotype by PCR		
<i>Trim27</i>	CTGCTTCACCAGCTGGGTCA CGTTG	GGAAACTCAGCAGAAGACTAC GGGCCACAGACGC

## Chapter 4

### 4. Results

---

#### 4.1 TNF- $\alpha$ -induced apoptosis is impaired in *Trim27*-deficient mice

To understand the physiological role of TRIM27, we generated *Trim27*-deficient (*Trim27*<sup>-/-</sup>) mice using homologous recombination in ES cells (**Figure 4.1**). Under pathogen-free conditions, *Trim27*<sup>-/-</sup> mice exhibited no obvious abnormality. We examined the abundance of CD4<sup>+</sup> and/or CD8<sup>+</sup> T cells, and also B220<sup>+</sup> B cells, and there was no difference between WT and *Trim27*<sup>-/-</sup> mice (data not shown).

As TRIM27 is a ubiquitin E3 ligase, and ubiquitination plays a role in the regulation of TNF- $\alpha$  signaling (67), we examined TNF- $\alpha$  signaling in *Trim27*<sup>-/-</sup> mice. We used a D-galactosamine (GalN) sensitized mouse model of liver injury in which TNF- $\alpha$  induces hepatocyte apoptosis in the presence of GalN [91]. GalN suppresses TNF- $\alpha$  survival signaling by inhibiting transcription in hepatocytes. WT mice treated with TNF- $\alpha$  and GalN died within 10 h, whereas 60% of *Trim27*<sup>-/-</sup> mice treated under the same conditions survived and lived even 24 h after injection (**Figure 4.2A**). TNF- $\alpha$ /GalN-induced liver injury was observed preferentially in WT mice (**Figure 4.2B**). The administration of TNF- $\alpha$  GalN induced higher elevation of serum AST and ALT levels in WT than in *Trim27*<sup>-/-</sup> mice (**Figure 4.2C**). Histological analysis of liver sections indicated that macrophages were infiltrated and hypostasis were evident in TNF- $\alpha$  GalN-treated WT liver (**Figure 4.2D**). TUNEL staining of liver sections and immunostaining with anti-cleaved caspase 3 showed that the rate of apoptosis was higher in WT hepatocytes than in *Trim27*<sup>-/-</sup> cells (**Figure 4.2E and 4.2F**). Furthermore,

WT liver homogenates contained higher caspase-3 and caspase-8 activities than *Trim27<sup>-/-</sup>* liver homogenates (**Figure 4.2G**). These results indicate that *Trim27<sup>-/-</sup>* hepatocytes are more resistant to the TNF- $\alpha$ /GalN-induced apoptosis than WT cells.

TNF- $\alpha$ -induced apoptosis was further examined in primary MEFs in the presence of cyclohexamide (CHX), which inhibits translation and thus inhibits TNF- $\alpha$  survival signaling. In WT MEFs, treatment with TNF- $\alpha$  or CHX alone did not inhibit cell viability, whereas the viability of MEFs treated with both TNF- $\alpha$  and CHX was significantly reduced (**Figure 4.3B**). By contrast, TNF- $\alpha$ /CHX treatment only slightly reduced the cell viability of primary *Trim27<sup>-/-</sup>* MEFs. To verify that the lack of TRIM27 was responsible for this effect, a *Trim27<sup>-/-</sup>* MEF cell line expressing exogenous TRIM27 was generated by infection with the TRIM27-expression retrovirus vector (**Figure 4.3A**). TNF- $\alpha$ /CHX reduced the cell viability of the *Trim27<sup>-/-</sup>* MEF cell line expressing TRIM27, similar to the effect on WT MEFs. When generation of cleaved caspase-3 was examined by Western blotting, TNF- $\alpha$ /CHX treatment induced higher level of cleaved caspase-3 in WT and *Trim27<sup>-/-</sup>* MEFs ectopically expressing TRIM27 than in *Trim27<sup>-/-</sup>* MEFs (**Figure 4.3C**).

#### **4.2 TRIM27 is not involved in TNF- $\alpha$ -induced survival signaling but required for TNF- $\alpha$ -induced apoptosis signaling**

As *Trim27<sup>-/-</sup>* mice showed the resistance against apoptosis so next we checked whether there is any change in the expression pattern of TNF- $\alpha$  receptor in WT and *Trim27<sup>-/-</sup>* mice. There was no difference in the expression level of TNF- $\alpha$  receptor between WT and *Trim27<sup>-/-</sup>* MEFs, as demonstrated by FACS and Western blotting analysis (**Figure**

**4.4A B**). In addition, other key factors for apoptosis, TRADD, TRAF2, RIP1, caspase-8, FADD, CYLD, were also expressed at similar levels in WT and *Trim27*<sup>-/-</sup> MEFs (**Figure 4.4B**).

To determine whether TRIM27 plays a role in TNF- $\alpha$  survival signaling, such as through NF- $\kappa$ B target gene expression, which results in the inhibition of apoptosis, the expression of typical survival-related genes including *cFLIP*, *cIAP2*, *A20*, and *ICAM* was assessed in the presence or absence of TNF $\alpha$ . The results showed that the expression levels of these genes were similar between WT and *Trim27*<sup>-/-</sup> primary MEFs (**Figure 4.4C**), indicating that TRIM27 does not affect TNF- $\alpha$  survival signaling. The NF- $\kappa$ B activity in WT and *Trim27*<sup>-/-</sup> MEFs was examined using EMSA. At various times after TNF- $\alpha$ /CHX treatment, similar levels of NF- $\kappa$ B activities were detected in WT and *Trim27*<sup>-/-</sup> MEFs (**Figure 4.4D**). *Trim27* mRNA level was also not significantly affected by TNF- $\alpha$  treatment (**Figure 4.5A**).

To investigate the role of TRIM27 in the complex II-dependent apoptosis pathway, the complex II formation was compared between WT and *Trim27*<sup>-/-</sup> MEFs. In WT cells, RIP1 and caspase-8 were co-immunoprecipitated with FADD 90 min after TNF- $\alpha$ /CHX treatment (**Figure 4.6**). However, the levels of RIP1 and caspase-8 co-immunoprecipitated with FADD were lower in *Trim27*<sup>-/-</sup> cells than in WT cells. These results suggest that TRIM27 is involved in the complex II-dependent apoptosis pathway, but not in the complex I-dependent survival signaling pathway.

To test whether TRIM27 has a general role in the apoptosis induced by various stimuli, the Fas-, TRAIL-, or etoposide-induced apoptosis was compared between WT and

*Trim27*<sup>-/-</sup> MEFs. There was no difference in the Fas-, TRAIL-, or etoposide-induced apoptosis between WT and *Trim27*<sup>-/-</sup> MEFs (**Figure 4.7**), suggesting that TRIM27 does not have the general role in the various types of apoptosis.

### **4.3 Localization of TRIM27 to mitochondria**

Our previous studies suggested that TRIM27 is localized both in the nucleus and in the cytosol [59]. As the data described above suggest that TRIM27 is involved in the TNF- $\alpha$ -induced apoptosis in the hepatocytes and MEFs, we examined the subcellular localization of TRIM27 in the human hepatocyte-derived cell line HepG2 and in MEFs. Immunostaining for TRIM27 in HepG2 cells showed a predominantly cytoplasmic pattern, in addition to weak nuclear signals (**Figure 4.8**). Cytoplasmic TRIM27 signals partly overlapped with those of MitoTracker, a mitochondrial-selective fluorescent label, indicating the partial localization of TRIM27 to mitochondria. Similar overlapping pattern of TRIM27 with MitoTracker was also observed in MEFs (**Figure 4.9 top panel**). Furthermore, TRIM27 subcellular localization was not affected by TNF- $\alpha$  or TNF- $\alpha$ /CHX treatment (**Figure 4.9**). These results were consistent with a prior study that showed that certain signaling molecules involved in TNF- $\alpha$  signaling, such as RIP1, localize to mitochondria [92].

To confirm the mitochondrial localization of TRIM27, the cytosolic lysate was separated by Nycodenz gradient centrifugation and the resulting fractions were analyzed by Western blotting with antibodies against TRIM27, mitochondria-specific HSP70 (mtHSP70), and PER5. TRIM27 was detected in small amounts in the mitochondrial fraction as shown with the anti-mtHSP70 antibody (**Figure 4.10A**), and in large

amounts in the peroxisome. Although the role of TRIM27 in the peroxisome is unknown, a recent report showed that the peroxisome is the signaling platform for antiviral innate immunity [93]. To further examine the mitochondrial location of TRIM27, the mitochondrial fraction was isolated from HepG2 cells transfected with the FLAG-TRIM27 expression vector and analyzed by Western blotting (**Figure 4.10C,D**), which showed that a significant amount of TRIM27 was present in mitochondria (**Figure 4.10D**). The isolated mitochondrial fraction was then treated with digitonin to disrupt the mitochondrial outer membrane or proteinase K, which degrades proteins on the surface of the outer membrane. The pellet fraction after digitonin treatment (mitoplast) contained TRIM27, suggesting that TRIM27 is localized in the mitoplast or tightly associated with the inner membrane. Furthermore, proteinase K digestion of the mitochondrial fraction resulted in the loss of the FLAG-tag containing N-terminal portion, suggesting that the N-terminal portion of TRIM27 is located on the outer mitochondrial membrane (**Figure 4.10E**).

#### **4.4 TRIM27 induces RIP1 deubiquitination**

TRIM25, an RBCC motif-containing protein, directly ubiquitinates RIG-I and promotes RIG-I-dependent interferon production in response to ds-RNA (52). We therefore hypothesized that the effect of TRIM27 on TNF- $\alpha$ -induced apoptosis may be mediated by ubiquitination of a regulatory factor. Of the several candidates examined, TRIM27 only affected the ubiquitination status of RIP1. However, contrary to its expected function as a Ub E3 ligase, TRIM27 deubiquitinated RIP1 (**Figure 4.11A**). In the co-immunoprecipitation assay, RIP1 was co-precipitated with TRIM27 (**Figure 4.11B**),

suggesting the interaction between TRIM27 and RIP1. Isolation of the cytosolic fraction of HepG2 cells using Nycodenz gradient centrifugation indicated that RIP1 also localized to mitochondria (**Figure 4.10B**), as reported previously [92]. We previously showed that TRIM27 shuttles between the cytoplasm and the nucleus via its nuclear export signal (NES) [59]. The TRM27 NES mutant, which is mainly localized in the nucleus, did not induce RIP1 deubiquitination (**Figure 4.11C**), indicating that deubiquitination of RIP1 is mediated by cytosolic TRIM27.

A polyubiquitin (poly-Ub) chain is generated through the formation of a link between one of the seven Lys side chains of Ub and the C-terminal Gly of another Ub. To determine the type of poly-Ub chain on RIP1 that is removed by TRIM27, we used Ub mutants in which all but one Lys residue are replaced by Arg. Expression of Ub mutants with active K27, K29, or K48 linkages resulted in the TRIM27-induced deubiquitination of RIP1, whereas K11- and K63-linked poly-Ub was removed only slightly by TRIM27 (**Figure 4.11D**). These results suggest that TRIM27 removes K11-, K27-, K29-, K48-, or K63-linked poly-Ub from RIP1. However, the poly-Ub chains bound to RIP1 may have a complex structure with various Lys linkages; therefore, the specificity of TRIM27 for a particular chain remains unclear.

#### **4.5 USP7 is required for the TRIM27-induced deubiquitination of RIP1**

To understand the mechanism underlying the deubiquitination of RIP1 by TRIM27, TRIM27-interacting proteins were identified by purifying the complex formed. HeLa cells were infected with a retrovirus encoding FLAG- and HA-tagged TRIM27 (FH-TRIM27), and a cell line expressing FH-TRIM27 was isolated. The

FH-TRIM27-containing complex was purified using anti-FLAG and anti-HA antibodies, and analyzed by SDS-PAGE. This complex contained a 120-kD band in addition to FH-TRIM27 (**Figure 4.12A**), which was identified by mass spectrometry as USP7 (also known as HAUSP, herpesvirus-associated ubiquitin-specific protease), a ubiquitin-specific protease. USP7 colocalized with TRIM27 in the cytoplasm and in the nucleus (**Figure 4.12B**), suggesting that these proteins interact. Furthermore, USP7 co-immunoprecipitated with TRIM27 in HepG2 cells transfected with the TRIM27 expression vector (**Figure 4.12C**).

To examine whether USP7 is needed for the TRIM27-induced deubiquitination of RIP1, we generated USP7-knockdown 293T cell lines by introducing an siRNA expression vector. Among multiple cell lines isolated, one clone (#44) expressed USP7 at a significantly low level (**Figure 4.13A**). When RIP1 was co-expressed with increasing amounts of TRIM27 in this cell line, RIP1 deubiquitination was not observed (**Figure 4.13B**), indicating that USP7 is required for the TRIM27-induced deubiquitination of RIP1. These results suggest that the TRIM27-USP7 complex binds to RIP1, resulting in its deubiquitination.

To further examine this interaction, we performed co-immunoprecipitation assays. Using 293T cell lysates, endogenous RIP1 and USP7 were co-immunoprecipitated with endogenous TRIM27 (**Figure 4.14A**). However, in 293T cells ectopically expressing the three proteins, TRIM27 was coimmunoprecipitated with USP7, but not with RIP1 (**Figure 4.14B**). When the USP7 mutant (C223A), in which the catalytic domain of the protease was disrupted by point mutation [94], was used, TRIM27 was

coimmunoprecipitated with both USP7 and RIP1 (**Figure 4.14C**). These results indicated that these three proteins interact, but RIP1 is immediately released after its deubiquitination by USP7. There was no difference in the *Usp7* mRNA level between WT and *Trim27*<sup>-/-</sup> MEFs (**Figure 4.5B**), indicating that TRIM27 regulates TNF- $\alpha$ -induced apoptosis not via regulating the USP7 level.

#### **4.6 Ubiquitination of USP7 by TRIM27 is required for the TRIM27-induced deubiquitination of RIP1**

To examine the role of TRIM27 in the TRIM27/USP7 complex-induced deubiquitination of RIP1, we investigated whether TRIM27 ubiquitinates USP7. Ubiquitination assays in 293T cells showed that the WT and the RING finger TRIM27 mutant, in which four Zn-binding residues of RING finger were replaced by Ala, ubiquitinated USP7, while the B-box mutant, in which four Zn-binding residues of B-box were replaced by Ala, did not (**Figure 4.15A,B**). Similar results were obtained using the USP7 catalytic domain mutant (C223A) (**Figure 4.15C**). As both the RING finger and the B-box mutants interacted with USP7 (**Figure 4.15D**), these results suggest that the B-box of TRIM27 acts as the catalytic domain for the ubiquitination of USP7, or that the B-box of TRIM27 recruits another Ub E3 ligase. To analyze the nature of the TRIM27-generated poly-Ub linkage on USP7, various Ub mutants in which all but one Lys residue were mutated to Arg were used for ubiquitination assays. TRIM27 catalyzed the Lys-linked polyubiquitination of USP7 in all cases (**Figure 4.15E**), suggesting that TRIM27 mediates the addition of poly-Ub chains to USP7 without selectivity for a particular linkage type.

As Lys-869 of USP7 is ubiquitinated [95], we examined the possible ubiquitination of USP7 at Lys-869. TRIM27 did not ubiquitinate the USP7-K869R mutant in which Lys-869 was mutated to Arg (USP7-K869R) (**Figure 4.16A**). Expression back of siRNA-resistant WT *USP7* mRNA in *USP7*-knockdown 293T cells recovered the TRIM27-induced RIP1 deubiquitination (**Figure 4.16B Left and 4.13B**), whereas overexpression of siRNA-resistant USP7-K869R mRNA did not (**Figure 4.16B, right**). These results indicate that the ubiquitination of USP7 by TRIM27 is required for the TRIM27-induced deubiquitination of RIP1.

When TRIM27 was expressed with USP7, the TRIM27 level was increased (**Figure 4.15B**). To further confirm, we examined the effect of increasing amounts of USP7 on the TRIM27 level and its ubiquitination. TRIM27 level was increased by USP7 in a dose-dependent manner, and the degree of TRIM27 ubiquitination per TRIM27 molecule decreased (**Figure 4.17**). These results suggest that USP7 stabilizes TRIM27 by removal of poly-Ub from TRIM27.

As TRIM27 is a ubiquitin E3 ligase, we have examined whether TRIM27 is autoubiquitinated via its RING finger domain. Ubiquitination degree of TRIM27 RING finger mutant was much lower than that of WT (**Figure 4.18A**). Next we determined the ubiquitinated sites of TRIM27 by mass spectrophotometry. Mutation of four ubiquitination sites (4KR) in TRIM27 dramatically decreased its ubiquitination (**Figure 4.18B**). Two TRIM27 mutants, RING finger and 4KR mutants, were localized exclusively and mainly in the nuclei, respectively (**Figure 4.18C**). Thus, autoubiquitination of TRIM27 may be required for its localization in the cytoplasm.

Furthermore, Ring finger mutant of TRIM27 was colocalized with USP7 in the nucleus, while 4KR mutant was not (**Figure 4.18C**). This may be due to the decreased interaction between 4KR mutant and USP7 (**Figure 4.18D**).

#### **4.7 Deubiquitination of RIP1 by the TRIM27-USP7 complex is required for TNF- $\alpha$ -induced apoptosis.**

To further confirm that USP7 plays a role in TNF- $\alpha$ -induced apoptosis, *Usp7* mRNA was down-regulated in immortalized MEF by using mouse siRNA. Western blot analysis showed that cells treated with siRNA sequence #407 expressed significantly lower levels of USP7 than control cells (**Figure 4.19A**). Down-regulation of USP7 made the cells resistant to TNF- $\alpha$ /CHX-induced apoptosis compared to control cells (**Figure 4.19B**). Furthermore, when WT MEFs were treated with the USP7 inhibitor HBX [96], cells were also resistant to TNF- $\alpha$ /CHX-induced apoptosis (**Figure 4.19C**). When generation of cleaved caspase-3 was examined by Western blotting, TNF- $\alpha$ /CHX treatment induced higher level of cleaved caspase-3 in control cells compared with *Usp7* knockdown or HBX treated MEFs (**Figure 4.19D**).

We next examined the ubiquitination of endogenous RIP1 in response to TNF- $\alpha$ /CHX treatment using WT, *Trim27*<sup>-/-</sup>, and *Usp7* knockdown MEF cell lines. The level of ubiquitinated RIP1 in *Trim27*<sup>-/-</sup> cells and USP7 knockdown cells was higher than in WT and control cells (**Figure 4.20A, B**). The difference in the degree of RIP1 ubiquitination between WT and *Trim27*<sup>-/-</sup> MEFs and between WT and *Usp7* knockdown MEFs was more evident at 30 and 120 min after TNF- $\alpha$ /CHX treatment than at 0 min after treatment. This is consistent with the results that TRIM27 is involved in the

TNF- $\alpha$ -induced apoptosis, but not in the TNF- $\alpha$ -induced NF- $\kappa$ B activation, which occurs at early timing after TNF- $\alpha$  stimulation. We also examined the K63-linked ubiquitination of RIP1. The level of K63-linked ubiquitination of RIP1 in *Trim27*<sup>-/-</sup> cells and USP7 knockdown cells was higher than in WT and control cells (**Figure 4.20A,B**). However, The difference in the degree of K63-linked RIP1 ubiquitination between WT and *Trim27*<sup>-/-</sup> MEFs and between WT and *Usp7* knockdown MEFs was much less compared with the difference in the total ubiquitination of RIP1. As there was no significant difference in the NF- $\kappa$ B activity between WT and *Trim27*<sup>-/-</sup> MEFs (**Figure 4.4D**), the K63-linked ubiquitinated RIP1 detected in *Trim27*<sup>-/-</sup> MEFs may contain the complex structure of poly-Ub together with K63-linked Ub, so that it may not function to activate the survival signaling. These results further support that the TRIM27/USP7 complex plays a role in TNF- $\alpha$ -induced apoptosis by mediating RIP1 deubiquitination.

#### **4.8. *Trim27*<sup>-/-</sup> mice are prone to STZ-induced diabetes**

Defect in apoptosis are associated with autoimmune diseases [78,108]. As *Trim27*<sup>-/-</sup> mice showed the resistance against apoptosis and previous genome-wide association studies in several autoimmune diseases and hundreds of common variants suggested an association between *TRIM27* polymorphisms and certain autoimmune diseases, such as type 1 diabetes [82], therefore, we examined the susceptibility of *Trim27*<sup>-/-</sup> mice to streptozotocin (STZ)-induced diabetes, an animal model of type 1 diabetes, which is thought to arise after an autoimmune attack on pancreatic islets involving T-cells and macrophages [97]. Assessment of blood glucose levels in *Trim27*<sup>-/-</sup> and WT mice

during 60 days after the first STZ injection showed that *Trim27*<sup>-/-</sup> mice had significantly higher blood glucose levels than WT mice at 14, 35, 42, 56, and 60 days (**Figure 4.21A**). Furthermore, *Trim27*<sup>-/-</sup> mice showed a significantly higher incidence of diabetes than WT mice (**Figure 4.21B**). These results correlated with the significant hypoinsulinemia detected in *Trim27*<sup>-/-</sup> mice at day 60 after the first STZ injection, which was greater than the reduction in insulin levels in WT mice (**Figure 4.21C**).

In addition, *Trim27*<sup>-/-</sup> mice showed a significant reduction of the insulin-positive areas per islet (**Figure 4.22A**). The reduced amount of insulin positive area in *Trim27*<sup>-/-</sup> mice might be due to increased apoptosis of pancreatic  $\beta$  cells as assessed by immunostaining of cleaved caspase 3 (**Figure 4.22B**). To investigate whether the increased sensitivity of *Trim27*<sup>-/-</sup> mice to the diabetogenic effects of STZ was associated with exaggerated insulinitis, pancreatic sections were histologically examined. The number of islets without infiltration was significantly lower in *Trim27*<sup>-/-</sup> mice than in WT mice, whereas the number of islets with clear infiltration was increased (**Figure 4.23A**). The clearly displayed infiltrated area of *Trim27*<sup>-/-</sup> mice were also strongly stained with anti-CD3 antibody, a general marker for lymphocyte (**Figure 4.23B**). These results indicated that *Trim27*<sup>-/-</sup> mice were susceptible to autoimmune diabetes.

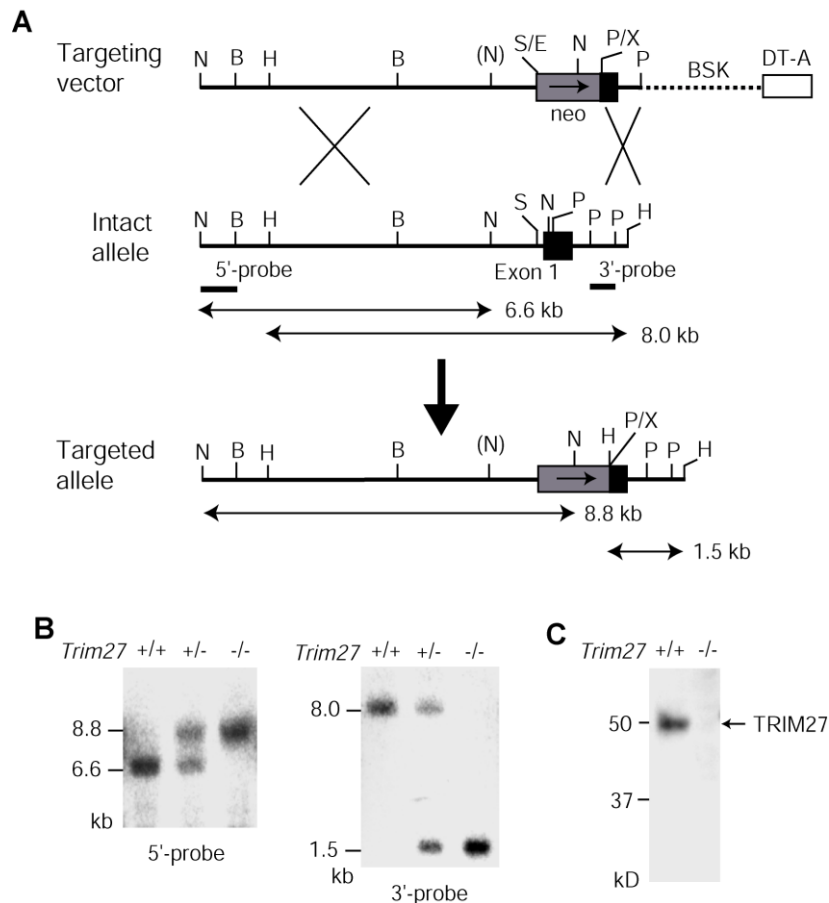


**Figure 4.1 Generation of *Trim27*-deficient (*Trim27*<sup>-/-</sup>) mice.** (A) Schematic representation of the mouse *Trim27* gene, the targeting vector, and the predicted disrupted allele. The probes used for Southern blot analyses are shown together with the predicted sizes of the hybridizing fragments. Restriction enzymes: B, *Bam*HI; E, *Eco*RI; H, *Hind*III; N, *Nco*I; P, *Pst*I; X, *Xho*I. Black and shaded boxes indicate the exon 1 region encoding the 5'-untranslated region and the N-terminal region of Trim27, which covers the RING finger, B box, and a part of the coiled-coil domain. In the targeting vector, the region encoding the N-terminal portion of Trim27, which includes the RING finger domain, was replaced by the PGK-neo cassette indicated by the gray box. (B) Southern blot analysis of genomic DNA extracted from the tails of wild-type (WT), *Trim27*<sup>+/-</sup>, and *Trim27*<sup>-/-</sup> mice. (Left panel) Genomic DNA digested with *Nco*I was hybridized with the 5' probe to yield 6.6-kb and 8.8-kb bands, representing the WT and targeted alleles, respectively. Note that one *Nco*I site surrounded by parenthesis in the targeting vector was disrupted. (Right panel) Genomic DNA digested with *Hind*III was hybridized with the 3' probe to yield 8.0-kb and 1.5-kb bands, representing the WT and targeted alleles, respectively. (C) Immunodetection of Trim27. Whole cell lysates from xx of WT, *Trim27*<sup>+/-</sup>, and *Trim27*<sup>-/-</sup> mice were used for immunoblotting with anti-Trim27 antibody. Equal amounts of total protein were loaded in each lane.

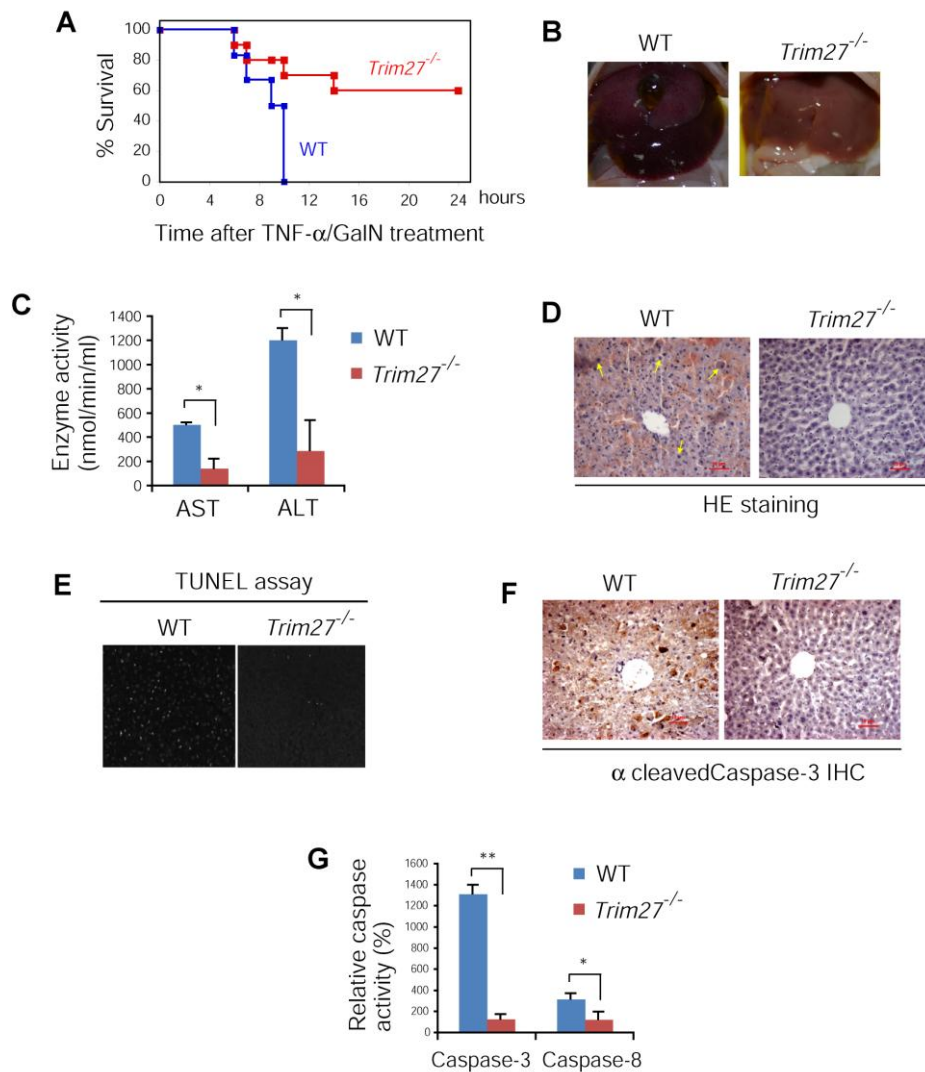


**Figure 4.2 TNF- $\alpha$  induced apoptosis is impaired in *Trim27* deficient mice** (A) Resistance of wild-type (WT) and *Trim27*<sup>-/-</sup> mice to TNF- $\alpha$  cytotoxicity. WT (n = 6) and *Trim27*<sup>-/-</sup> (n = 10) mice were treated with TNF- $\alpha$  (20  $\mu$ g/kg) and GalN (700 mg/kg) and their mortality was monitored over next 24 h. (B) The liver of mouse 6 h after TNF- $\alpha$ /GalN injection. (C) Serum AST and ALT levels were determined 4 h after TNF- $\alpha$ /GalN injection. Data are averages  $\pm$  SEM (n = 3 for WT, 4 for *Trim27*<sup>-/-</sup> mice). \*, p < 0.05. (D-F) Histological analysis (H&E staining) (D), TUNEL staining (E), and anti-cleaved caspase-3 immunostaining (F) were performed on liver sections 6 h after TNF $\alpha$ /GalN injection. Infiltrated macrophages (yellow arrows) and hypostasis are observed in WT section. Scale bar, 10  $\mu$ m. (G) Activities of caspase-3 and caspase-8 in liver homogenate of WT and *Trim27*<sup>-/-</sup> prepared at 6 h after TNF $\alpha$ /GalN injection. Data are averages  $\pm$  SEM (n = 3). \*, p < 0.05.

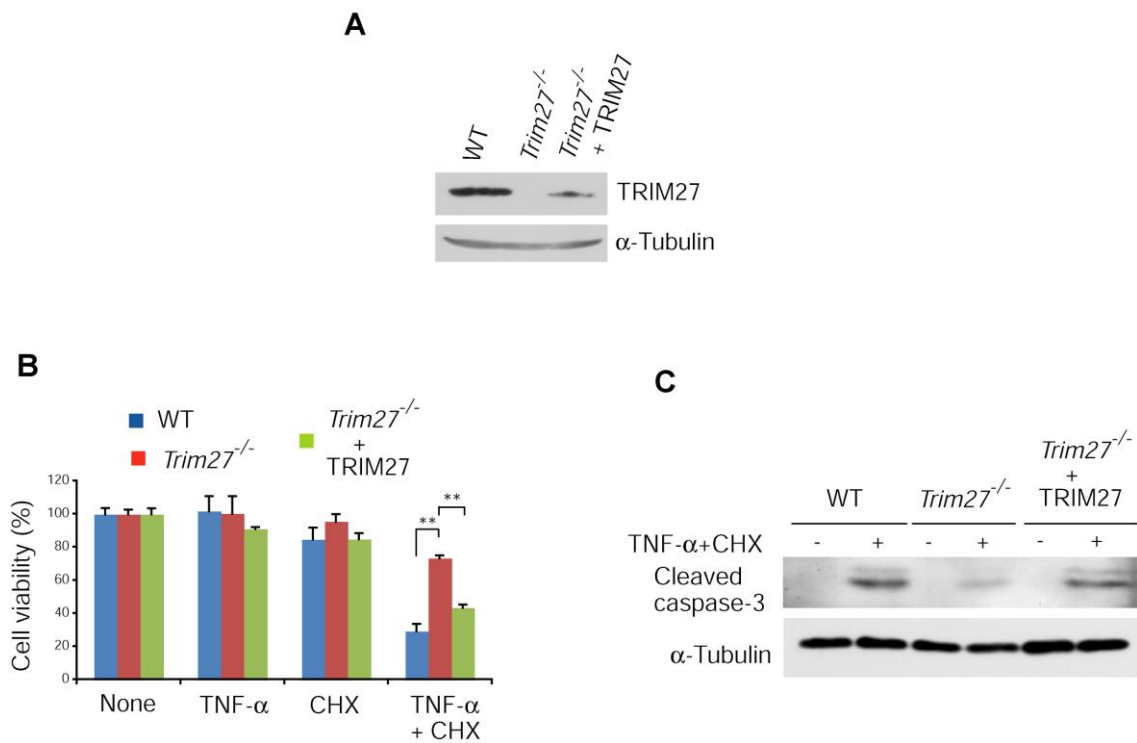


**Fig 4.3 *Trim27*<sup>-/-</sup> MEFs are resistant to TNF $\alpha$  induced apoptosis.** (A) Expression of TRIM27 in immortalized MEFs. Immortalized MEFs from WT and *Trim27*<sup>-/-</sup> mice analyzed by Western blotting against TRIM27. The *Trim27*<sup>-/-</sup> immortalized MEF cell line expressing exogenous TRIM27 was established by infection with a TRIM27-expression retrovirus vector, and was also used. Equal amounts of total protein were loaded in each lane. (B) WT and *Trim27*<sup>-/-</sup> MEFs ( $1 \times 10^4$  cells) were plated on 96-well plates and treated with TNF- $\alpha$  (10 ng/mL), or CHX alone (1  $\mu$ g/mL), or in combination with TNF- $\alpha$  (10 ng/mL) and CHX (1  $\mu$ g/mL). Six hours after treatment, cell viability was measured. Average value (n = 5) relative to the non-treated cells is shown with SD. \*\*, p < 0.01. The *Trim27*<sup>-/-</sup> MEF cell line expressing exogenous TRIM27 was used as the control. (C) Cleaved caspase-3 was determined by immunoblot analysis of MEFs lysates prepared at 3 h after TNF- $\alpha$ /CHX addition.

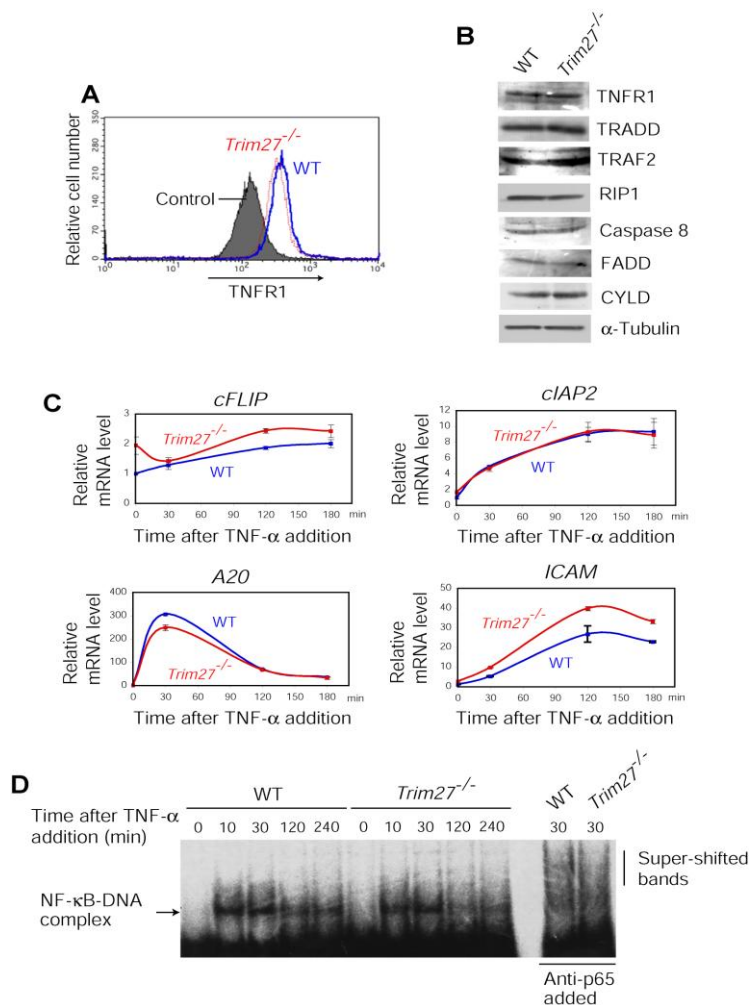


**Figure 4.4 TRIM27 is not involved in TNF- $\alpha$ -induced survival signaling.** (A) TNFR1 expression. TNFR1 expression in WT and *Trim27*<sup>-/-</sup> MEFs was examined by flow cytometry. (B) Expression of TNF- $\alpha$  signaling components. Expression levels of indicated proteins were compared between WT and *Trim27*<sup>-/-</sup> MEFs by Western blotting.  $\alpha$ -Tubulin was used as a control. (C) Analysis of the expression of survival-related genes. Primary MEFs from WT and *Trim27*<sup>-/-</sup> mice were treated with TNF- $\alpha$  (20 ng/ml), and the expression levels of four NF- $\kappa$ B-dependent survival-related genes were analyzed by qRT-PCR. Mean values  $\pm$  S.D. (n = 3) is shown. (D) EMSA of NF- $\kappa$ B after treatment of MEFs with TNF- $\alpha$ . TNF- $\alpha$  (20 ng/ml) was added to the culture of WT and *Trim27*<sup>-/-</sup> MEFs, and nuclear extracts were prepared at the indicated time. EMSA was performed using the NF- $\kappa$ B DNA probe. Where indicated, anti-p65 antibodies were added, so that supershift of NF- $\kappa$ B-DNA band was observed.

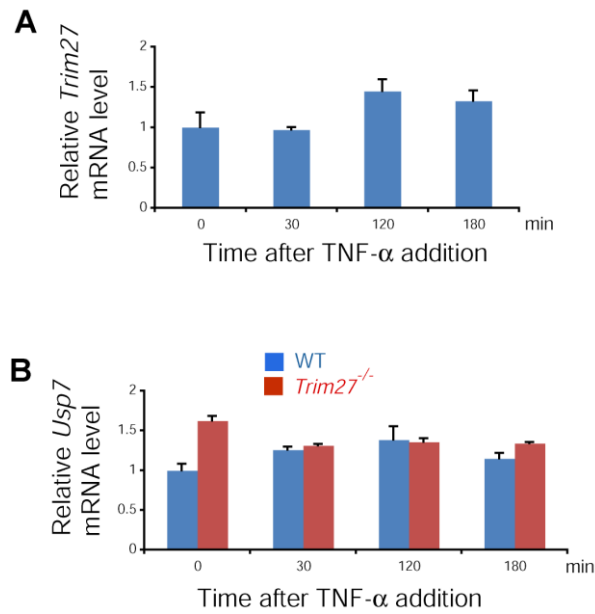


**Figure 4.5** Effect of TNF- $\alpha$  treatment on *Trim27* and *Usp7* expression. Primary MEFS from WT or *Trim27*<sup>-/-</sup> mice were treated with TNF- $\alpha$  (20 ng/ml), and expression levels of *Trim27* (A) or *Usp7* (B) were analyzed by qRT-PCR. Mean values  $\pm$  S.D. (n = 3) is shown.



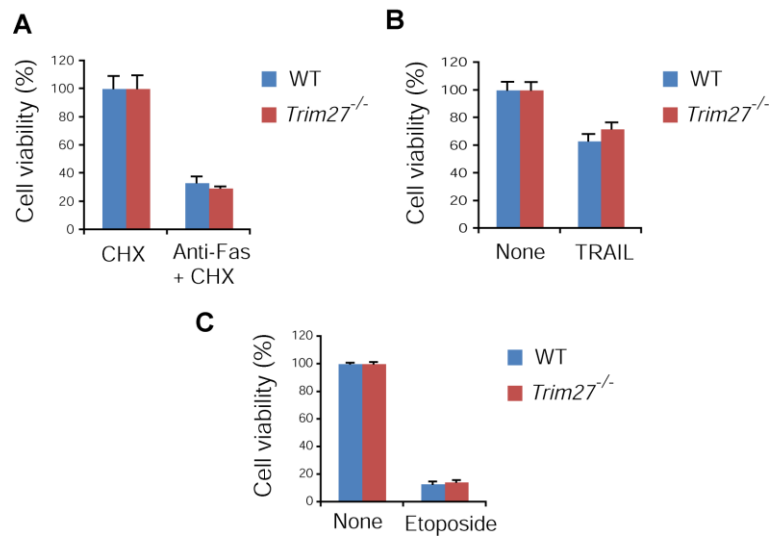


**Figure 4.7 FAS-, TRAIL-, or etoposide-induced apoptosis.** WT and *Trim27*<sup>-/-</sup> MEFs were treated with Anti-Fas antibody (5  $\mu$ g/ml) and CHX (1  $\mu$ g/ml) (A), Recombinant human TRAIL (100 ng/ml in conjugation with 2  $\mu$ g/ml enhancer antibody) (B) or etoposide (200  $\mu$ M) (C). 24 h (TRAIL/FAS) or 36 hr (Etoposide) after treatment cell viability was measured. Average of values relative to the non-treated cells is shown with SD.

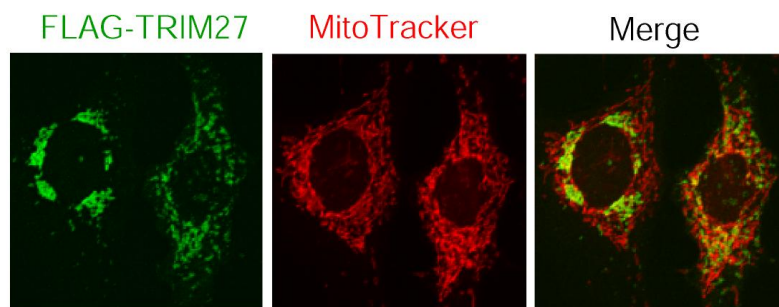


**Figure 4.8 Subcellular localization of TRIM27.** HepG2 cells were transfected with a FLAG-TRIM27 expression vector, incubated with Mitotracker, fixed with 1% paraformaldehyde, and incubated with an anti-FLAG antibody. After treatment with the corresponding secondary antibodies, fluorescence signals were visualized with a laser confocal microscope. The far right panel shows the merged signals for Mitotracker (red) and TRIM27 (green)

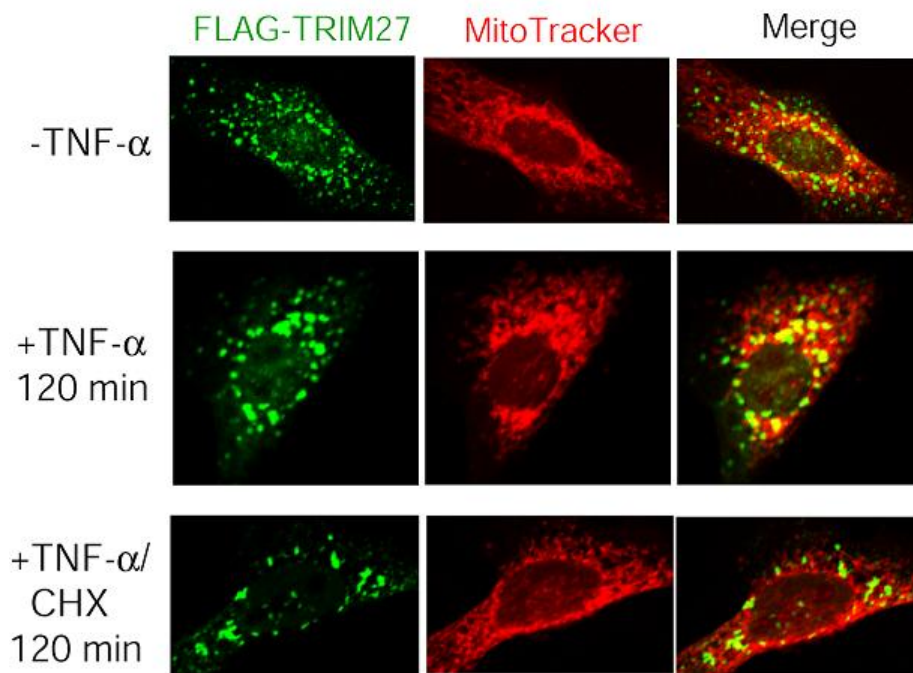


**Figure 4.9 Localization of TRIM27 is not affected by TNF $\alpha$  in MEF.** Immortalized MEFs were transfected with FLAG-TRIM27 expression vector, and treated with TNF- $\alpha$  (20 ng/ml) for indicated time. Cells were incubated with Mitotracker, fixed with 1% paraformaldehyde, and incubated with anti-FLAG antibody. After the treatment of the secondary antibodies, fluorescence signals in cells were visualized under the laser confocal microscope. The signals for Mitotracker (red) and TRIM27 (green) were merged on the right most panel.

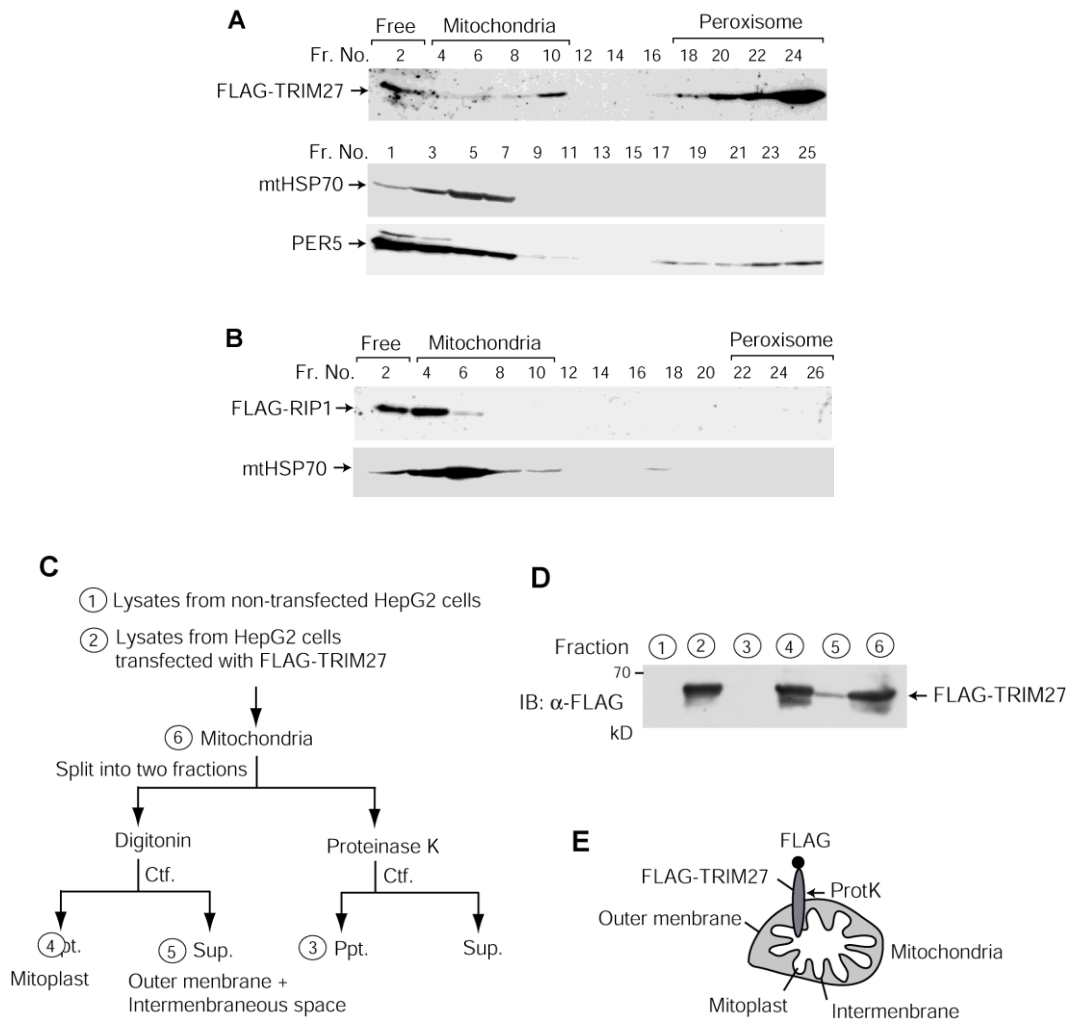


**Fig 4.10 Biochemical proof for mitochondrial localization of TRIM27.** (A) Subcellular fractionation experiments. Cytosolic fractions of immortalized WT MEFs transfected with FLAG-TRIM27 expression plasmids were subjected to Nycodenz gradient fractionation. The levels of FLAG-TRIM27, the mitochondrial marker mtHSP70, and the peroxisome marker PER5 in each fraction were analyzed by immunoblotting. (B) Localization of RIP1 in mitochondria. Cytosolic fractions of immortalized WT MEFs transfected with FLAG-RIP1 expression plasmids were subjected to Nycodenz gradient fractionation as described above. The levels of FLAG-RIP1 and mtHSP70 in each fraction were analyzed by immunoblotting. (C) Mitochondria were purified from HepG2 cells transfected with the FLAG-TRIM27 expression vector, and treated with digitonin or proteinase K. Fractions such as the mitoplast were separated by centrifugation. (D) Equivalent amounts of each fraction were analyzed by SDS-PAGE, followed by Western blotting with anti-FLAG antibody. (E) The localization of TRIM27 in mitochondria, which was suggested by the data, is schematically shown below.

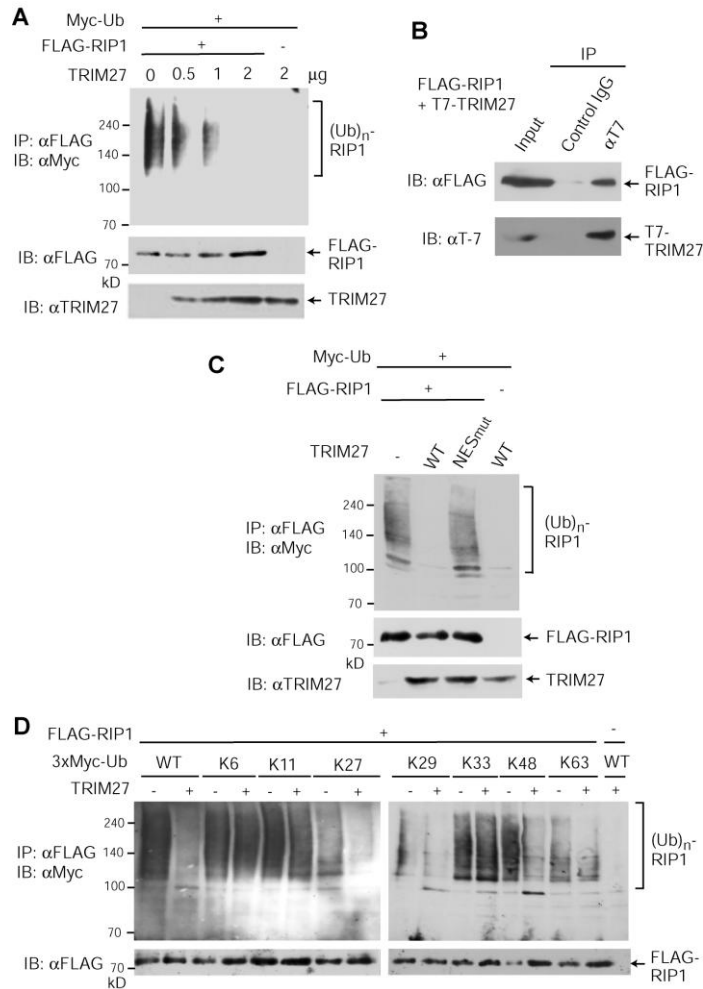


**Figure 4.11 TRIM27 deubiquitinates RIP1.** (A) Deubiquitination of RIP1 by TRIM27. HEK293T cells were transfected with the FLAG-RIP1 expression vector or control empty vector, together with the Myc-Ub expression vector and increasing amounts of the TRIM27 expression vector. Upper panel: cell lysates were immunoprecipitated with an anti-FLAG antibody and immunocomplexes were analyzed by Western blotting against anti-Myc. Lower panel: cell lysates were probed against an anti-FLAG antibody. (B) Co-immunoprecipitation of TRIM27 with RIP1. Upper panel: HEK293T cells were transfected with vectors expressing FLAG-RIP1 and T7-TRIM27, and cell lysates were immunoprecipitated with anti-T7 antibody or control IgG, followed by Western blotting with anti-FLAG. Asterisk indicates a non-specific band. Lower panel: lysates were analyzed by Western blotting with anti-TRIM27. (C) RIP1 deubiquitination is impaired with the TRIM27 NES mutant. Experiments were performed as described in (a) by substituting the NES mutant of TRIM27, which cannot be exported from the nucleus, for WT TRIM27. (D) Analysis of the ubiquitin chains removed from RIP1. Experiments were performed as described in (a), except for the use of different vectors expressing the indicated ubiquitin mutants instead of WT ubiquitin

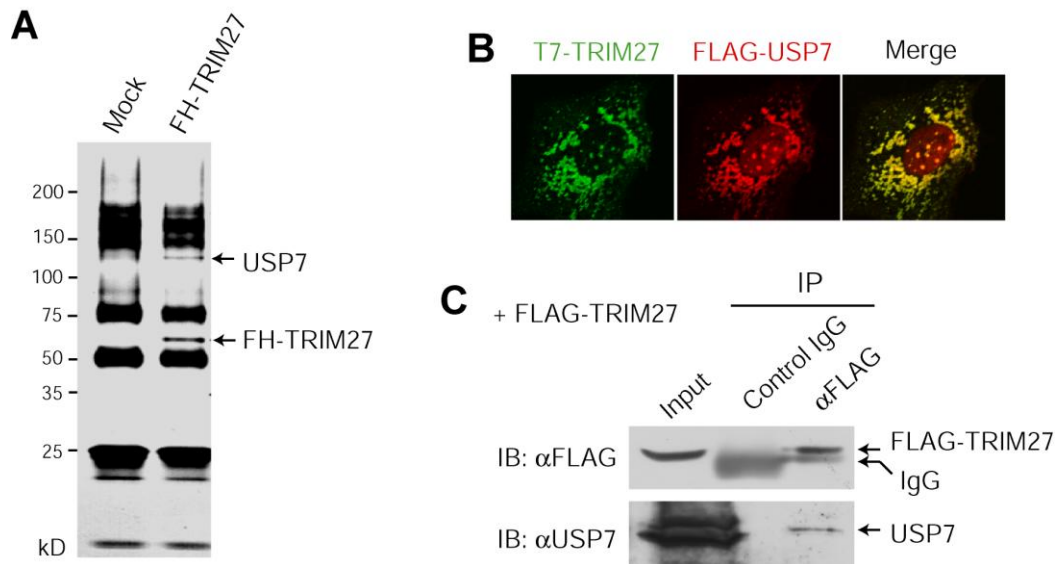


**Figure 4.12 TRIM27 forms a complex with USP7** (A) Formation of a complex between TRIM27 and USP7. The TRIM27 complex was purified from HeLa cells expressing FLAG- and HA-tagged TRIM27 (FH-TRIM27) or control HeLa cells (mock) using anti-FLAG and anti-HA antibodies, and analyzed by SDS-PAGE followed by silver staining. Mass spectrometry analysis identified the two bands indicated by arrows as USP7 and FH-TRIM27. (B) Co-localization of TRIM27 and USP7. HepG2 cells were transfected with vectors expressing T7-tagged TRIM27 and FLAG-USP7, and immunostained with anti-T7 and anti-FLAG antibodies. After treatment with the corresponding secondary antibodies, fluorescence signals were visualized under a laser confocal microscope. Merged signals for T7-TRIM27 and FLAG-USP7 are shown on the far right panel. (C) Co-immunoprecipitation of TRIM27 and USP7. HEK 293T cells were transfected with the FLAG-TRIM27 expression vector or control empty vector, and cell lysates were immunoprecipitated with anti-FLAG antibody or control IgG. The immunocomplexes were subjected to Western blotting using anti-FLAG or anti-USP7 antibodies.

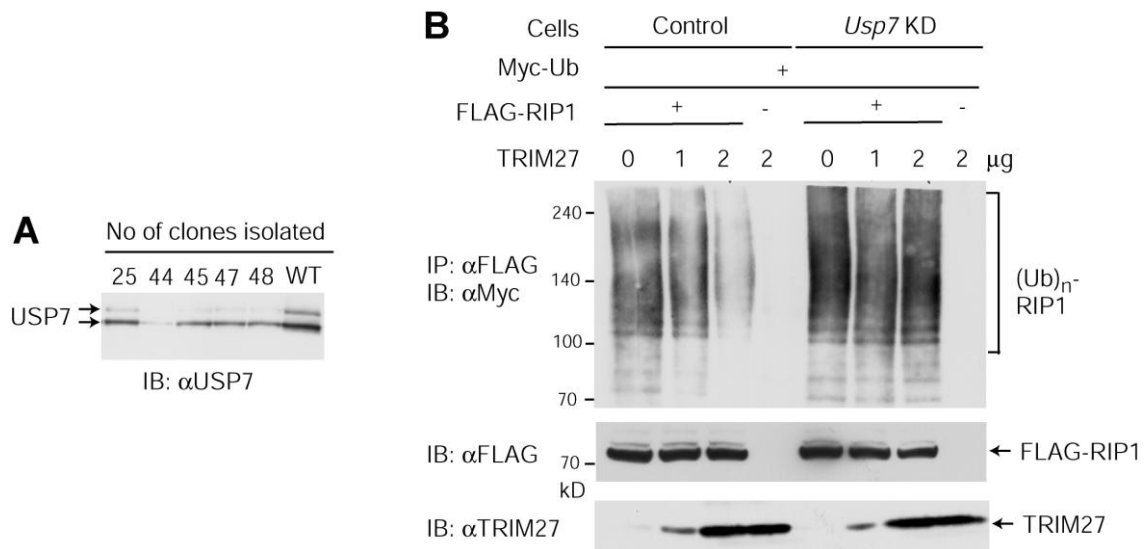


**Fig 4.13 USP7 is required for the TRIM27-induced deubiquitination of RIP1.** Generation of USP7 knockdown 293T cells. The 293T cell transfectants expressing the small hairpin RNA against the *USP7* gene were isolated, and cell lysates were analyzed by Western blotting against anti-USP7. Equal amounts of total protein were loaded in each lane. (E) Knockdown of USP7 abrogates the TRIM27-induced deubiquitination of RIP1. Experiments were performed as described in Figure 3a, except for the use of USP7-knockdown cells (#44) instead of parental 293T cells.

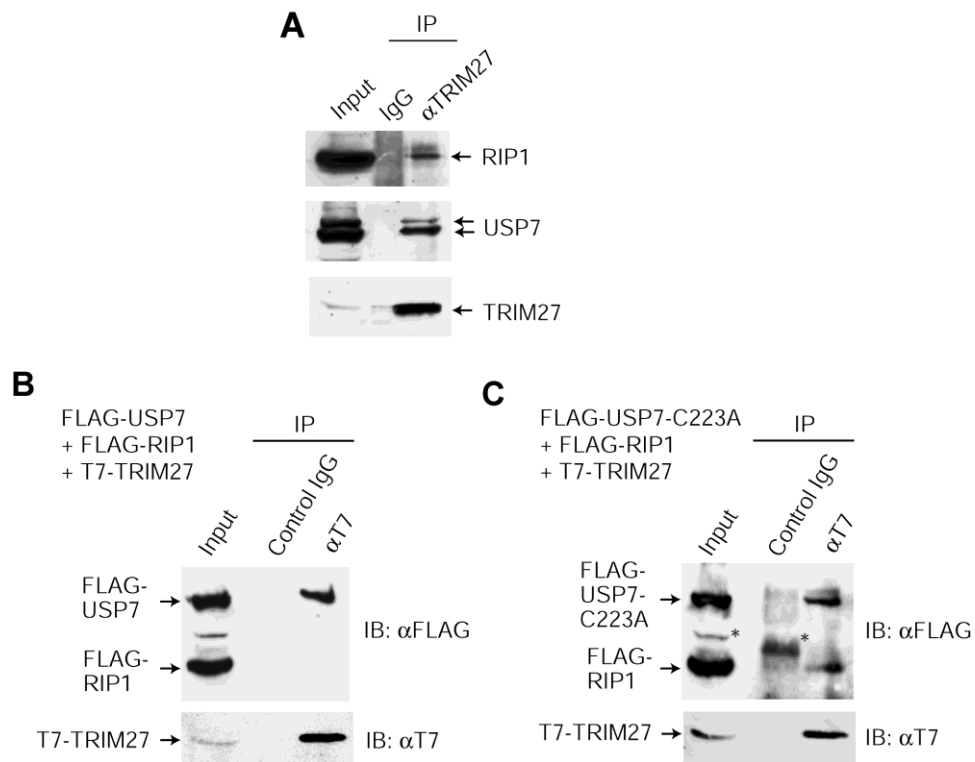


**Figure 4.14 TRIM27, RIP1 and USP7 forms a complex.** (A) Coimmunoprecipitation of endogenous TRIM27 with RIP1 and USP7. Whole cell lysates from HEK 293T cells were immunoprecipitated with anti-TRIM27 or control IgG, and the immunocomplexes were analyzed by SDS-PAGE, followed by Western blotting with anti-RIP1, anti-USP7, or anti-TRIM27. (B and C) The RFP-USP7 complex transiently interacts with RIP1. HEK 293T cells were co-transfected with the T7-RFP and FLAG-RIP1 expression vectors and the WT (B) or catalytic domain mutant (C223A) (C) of FLAG-USP7. Upper panel: lysates were immunoprecipitated with anti-T7 or control IgG and analyzed by Western blotting against anti-FLAG. Lower panel: lysates were subjected to Western blotting against anti-T7. Asterisk indicates a non-specific band.

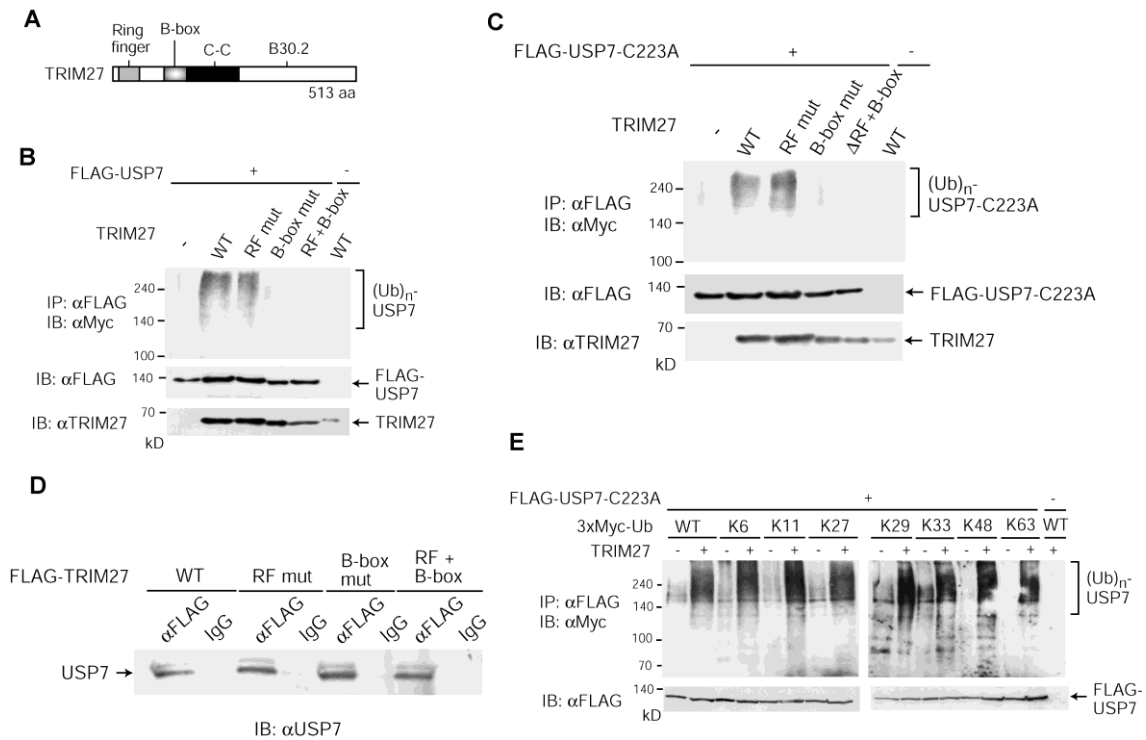


**Fig 4.15 TRIM27 ubiquitinates the USP7.** (A) Domain structure of TRIM27. (B) TRIM27 ubiquitinates USP7 via its B-box domain. HEK293T cells were co-transfected with FLAG-USP7 and Myc-ubiquitin expression vectors and a plasmid for the expression of the indicated form of TRIM27. Upper panel: cell lysates were immunoprecipitated with anti-FLAG followed by immunoblotting against anti-Myc. Lower panel: lysates were analyzed by Western blotting with anti-FLAG or anti-TRIM27 antibodies. (C) Ubiquitination of USP7 by TRIM27 was examined as described in (B), except that the USP7 mutant, in which Cys-223 in the catalytic domain was mutated to Ala, was used instead of WT USP7. (D) Co-immunoprecipitation of USP7 and various forms of TRIM27. HEK293T cells were transfected with a vector expressing the indicated form of FLAG-TRIM27, and cell lysates were immunoprecipitated with anti-FLAG antibody or control IgG. The immunocomplexes were subjected to Western blotting using anti-FLAG or anti-USP7 antibodies (E) Analysis of polyubiquitin chains attached to USP7. Ubiquitination of the USP7 catalytic mutant C223A, which lacks ubiquitin protease activity, was examined as described in (c), except for the use of the USP7-C223A mutant instead of WT USP7 and the indicated mutant ubiquitin instead of WT ubiquitin.

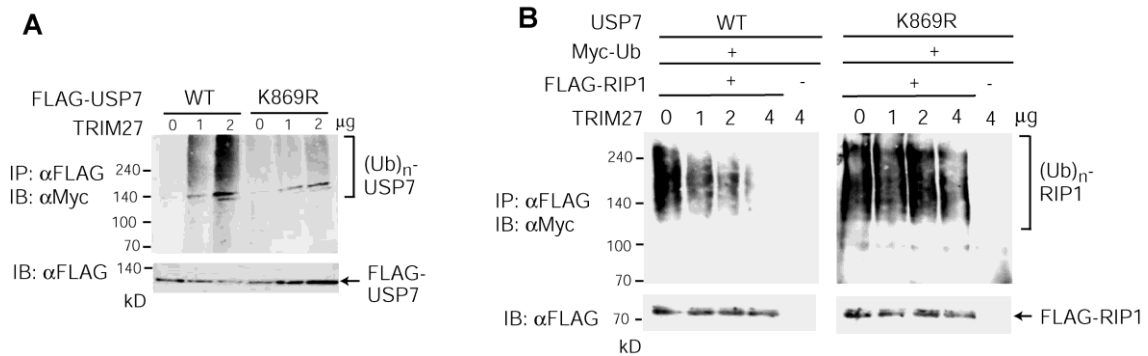


**Figure 4.16 TRIM27 induces RIP1 deubiquitination by ubiquitinating and activating USP7.** (A) USP7 Lys-869 is ubiquitinated by TRIM27. HEK293T cells were transfected with an expression vector for FLAG-linked WT or the USP7 K869R mutant, in which Lys-869 is mutated to Arg, together with Myc-ubiquitin and TRIM27 expression vectors. Upper panel: cell lysates were immunoprecipitated with anti-FLAG antibody, followed by immunoblotting against anti-Myc. Lower panel: lysates were analyzed by Western blotting with anti-FLAG antibody. (B) TRIM27 ubiquitination of USP7 at Lys-869 is required for TRIM27-induced RIP1 deubiquitination. The USP7-knockdown HEK293T cells were transfected with the FLAG-RIP1 expression vector, together with vectors expressing Myc-ubiquitin and WT or the K869R USP7 mutant, which was resistant to USP7 shRNA, and increasing amounts of the TRIM27 expression vector. Upper panel: Cell lysates were immunoprecipitated with anti-FLAG antibody, and the immunocomplexes were subjected to Western blotting with anti-Myc antibody. Lower panel: Lysates were analyzed by Western blotting with anti-FLAG or anti-USP7 antibodies.

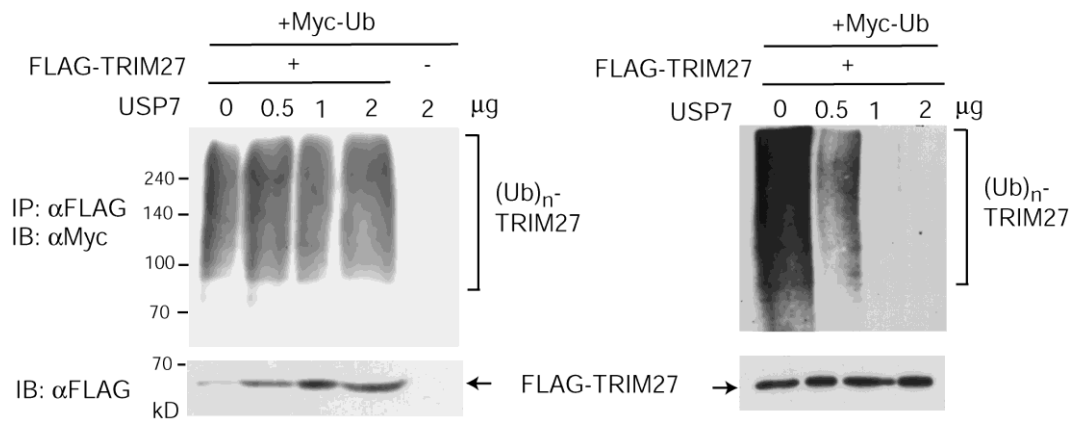


**Fig 4.17 Effect of USP7 on TRIM27 ubiquitination.** HEK293T cells were transfected with the FLAG-TRIM27 expression vector or control empty vector, together with the Myc-Ub expression vector and increasing amounts of the USP7 expression vector. (Left) Upper panel: Cell lysates were immunoprecipitated with anti-FLAG antibody, and the immunocomplexes were subjected to Western blotting with anti-Myc antibody. Lower panel: Lysates were analyzed by Western blotting with anti-FLAG antibody. (Right) The amount of sample per lane was adjusted to contain similar level of FLAG-TRIM27, and analyzed as described above.

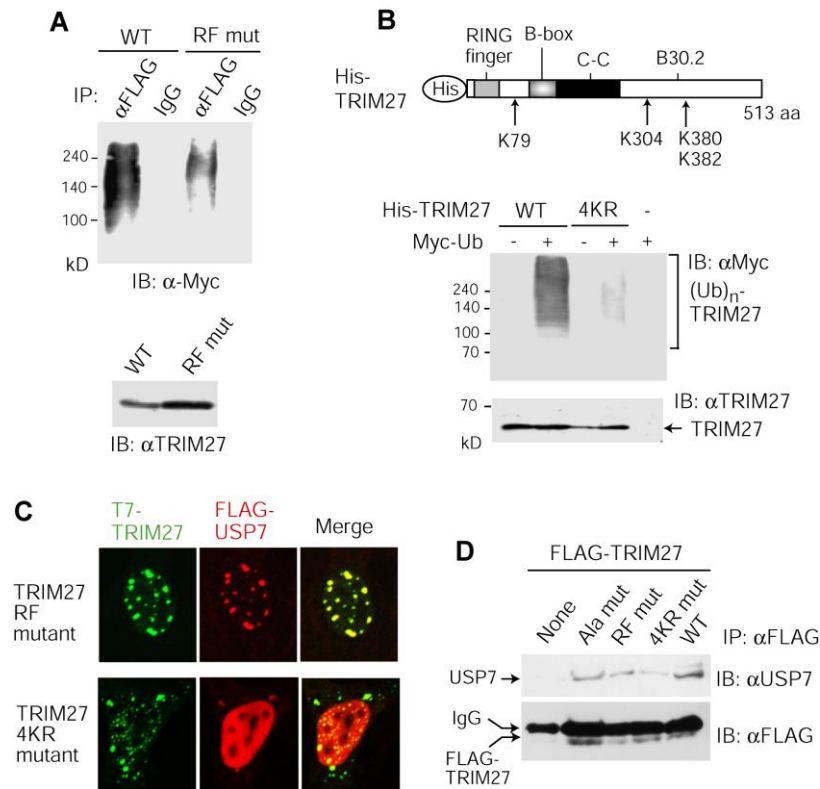


**Fig 4.18 Autoubiquitination of TRIM27.** (A) HEK293T cells were transfected with the vector to express WT or RING finger mutant (RF), or control empty vector, together with the Myc-Ub expression vector. Upper panel: cell lysates were immunoprecipitated with anti-FLAG antibody, and the immunocomplexes were subjected to Western blotting with anti-Myc antibody. Lower panel: lysates were analyzed by Western blotting with anti-TRIM27 antibody. (B) HepG2 cells were transfected with the vector to express His-tagged WT or 4KR mutant of TRIM27, in which four ubiquitination sites, Lys-79, Lys-304, Lys-380, and Lys-382, were replaced by Arg, or control empty vector, together with the Myc-Ub expression vector. Upper panel: His-tagged TRIM27 was purified using cobalt-resin, and was subjected to Western blotting with anti-Myc antibody. lower panel: Lysates were analyzed by Western blotting with anti-TRIM27 antibody. (C) Co-localization of TRIM27 mutants and USP7. HepG2 cells were transfected with vectors expressing T7-tagged TRIM27 mutants and FLAG-USP7, and immunostained with anti-T7 and anti-FLAG antibodies. After treatment with the corresponding secondary antibodies, fluorescence signals were visualized under a laser confocal microscope. (D) Co-immunoprecipitation of TRIM27 mutants with USP7. HEK293T cells were transfected with the vector to express FLAG-tagged TRIM27 mutants. In the Ala mutant, putative phosphorylation sites (Ser-476, 478, and 482) of TBK-1 and IKK $\epsilon$  were replaced by Ala. Whole cell lysates from transfected cells were immunoprecipitated with anti-FLAG, and the immunocomplexes were analyzed by Western blotting with anti-USP7 or anti-FLAG.

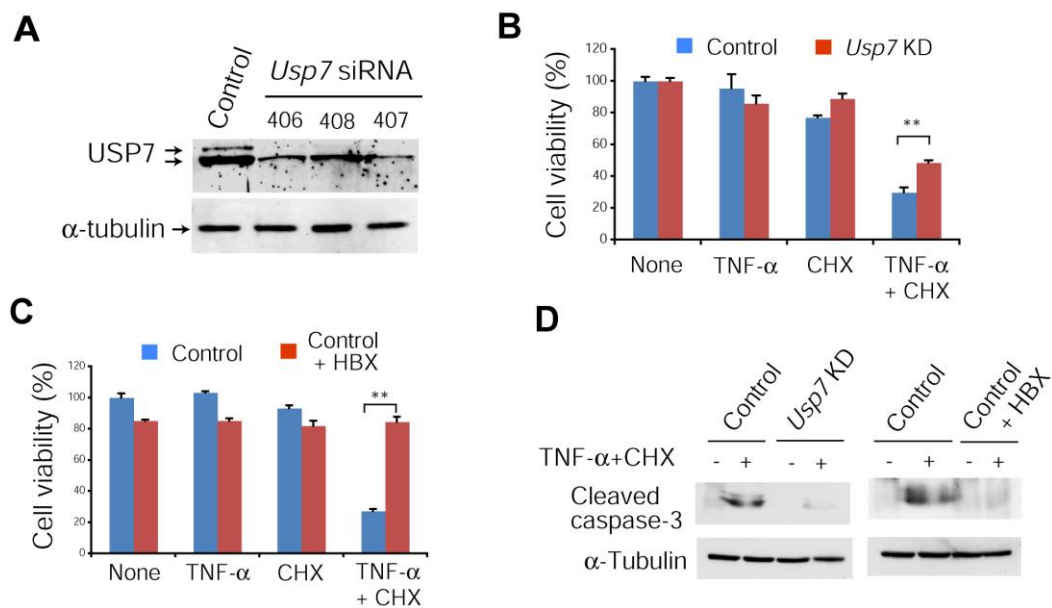


**Figure 4.19 USP7 is required for TNF- $\alpha$  induced apoptosis** (A) Knockdown of *Usp7* using siRNA in immortalized MEF. Three different sequences of mouse *Usp7* siRNA were transfected, and cell lysates were analyzed by Western blotting with anti-USP7 (upper) or anti-tubulin (lower) antibodies. (B and C) USP7 is involved in TNF- $\alpha$ /CHX-induced apoptosis. Cell viability was examined as described in Figure II using control immortalized MEFs, *Usp7*-knockdown cells (B), and WT cells pretreated with the USP7 inhibitor HBX 41,108 (20  $\mu$ M) for 4 h (C). Experiments were repeated three times, and average value relative to the non-treated cells is shown with SD. \*\*,  $p < 0.01$ . (D) Cleaved caspase-3 was determined by immunoblot analysis of MEFs lysates prepared at 3.5 h after TNF- $\alpha$ /CHX addition.

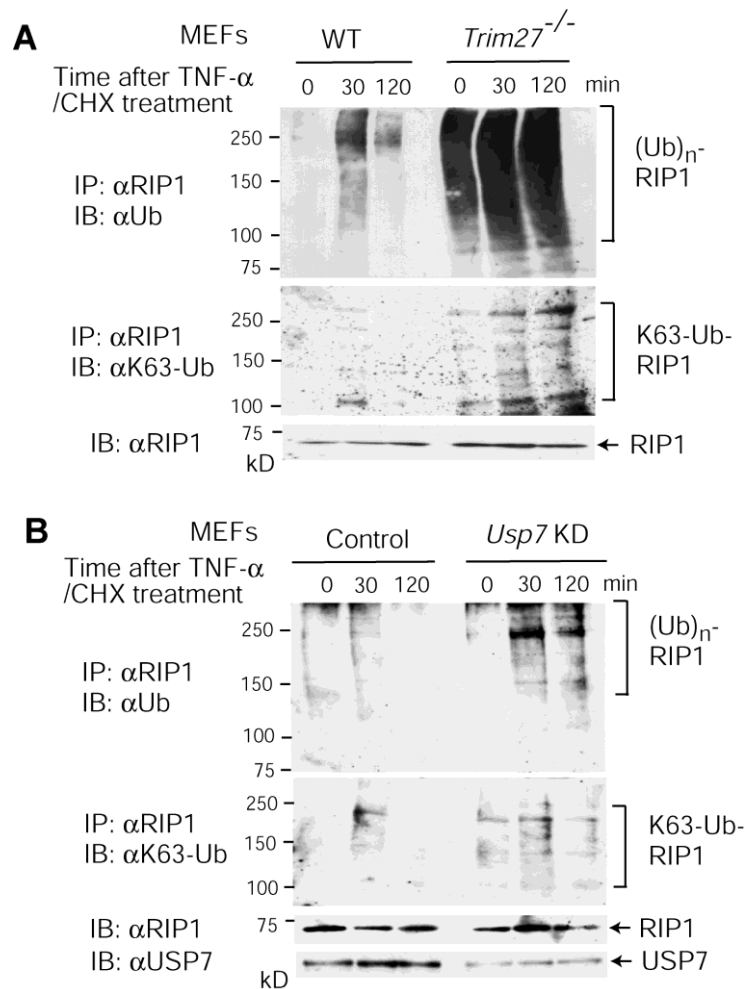


**Figure 4.20 TRIM27-USP7 regulation of RIP1 ubiquitination in the presence of TNF $\alpha$  and CHX.** (A and B) Ubiquitination of endogenous RIP1 after TNF $\alpha$ /CHX treatment. Immortalized WT, *Trim27*<sup>-/-</sup> (A) or *Usp7*-knockdown (B) MEFs were treated with TNF- $\alpha$  (10 ng/ml) and CHX (1 $\mu$ g/ml) for the indicated time. Endogenous RIP1 was immunoprecipitated and analyzed by immunoblotting with anti-Ub (upper panel) or anti-K63-linked Ub (lower panel) antibody. Lysates were also analyzed by Western blotting with anti-RIP1 or anti-USP7 antibodies.

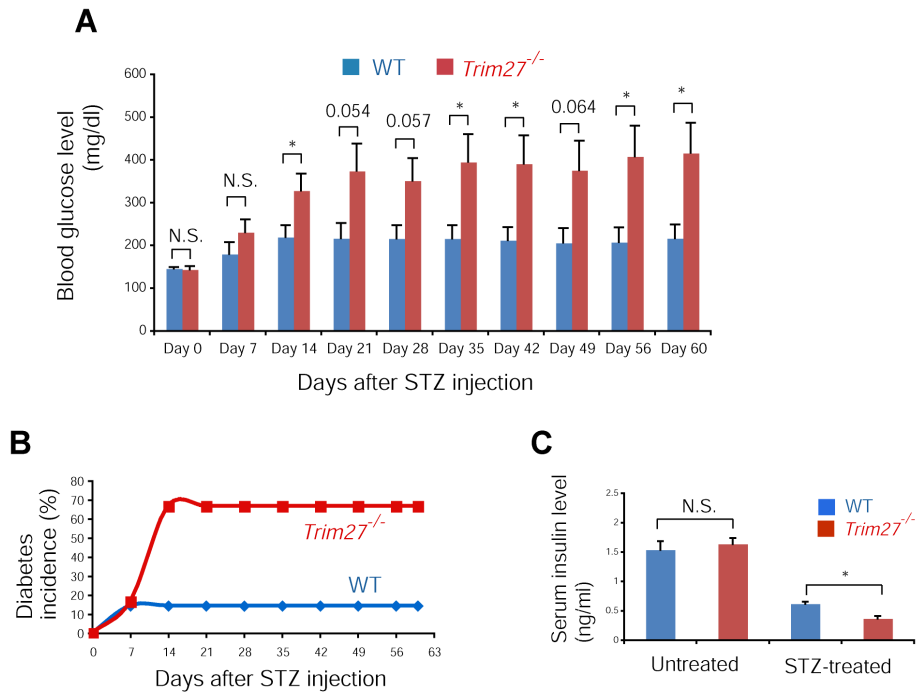


**Figure 4.21** *Trim27*<sup>-/-</sup> mice are prone to STZ-induced diabetes. (A) Blood glucose levels of WT and *Trim27*<sup>-/-</sup> mice after streptozotocin (STZ) injection. Mice were injected intraperitoneally with STZ, and blood glucose level was measured weekly. Mean value  $\pm$  S.E.M. (WT, n = 6; *Trim27*<sup>-/-</sup>, n = 7) is shown. (B) Incidence of STZ-induced diabetes. WT (n = 6) and *Trim27*<sup>-/-</sup> (n = 7) mice were injected with multiple low doses of STZ, and the blood glucose level was monitored weekly in non-fasted animals using a glucometer. Animals were considered diabetic when the blood glucose level exceeded 300 mg/dL. (C) Serum insulin levels of control (no treatment) and STZ-treated mice at 60 days after the first STZ injection. Each bar represents the mean  $\pm$  SEM. \*, p < 0.05; N.S., no significant difference.

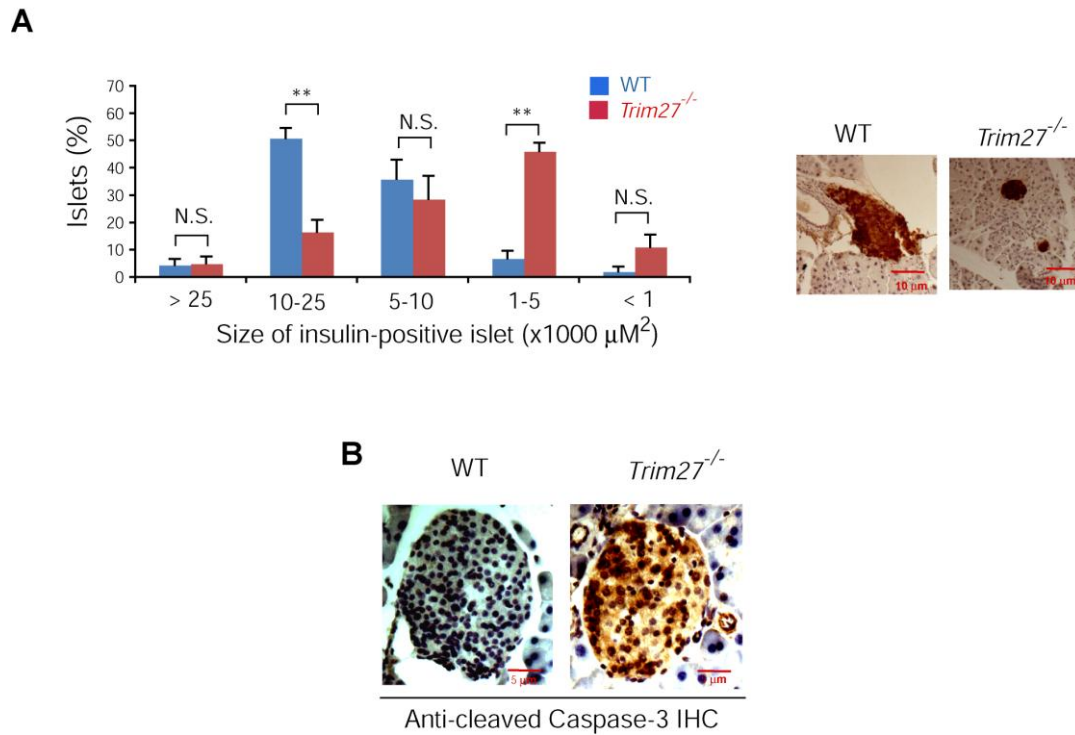


**Figure 4.22 Reduced  $\beta$ -cell mass and increased apoptosis in STZ induced diabetic *Trim27*<sup>-/-</sup> mice.** (A) Decreased  $\beta$ -cell mass in *Trim27*<sup>-/-</sup> mice at 60 days after the first STZ injection. Pancreatic sections were immunostained with anti-insulin antibody, and the size of insulin-positive islets and its frequency were measured. Islet size was averaged from six WT and seven *Trim27*<sup>-/-</sup> mice, using three sections from each animal. The average frequency  $\pm$  SEM are shown as a bar graph (left), and typical sections are shown (right). \*\*,  $p < 0.01$ ; N.S., no significant difference. Scale bar 10  $\mu$ m. (B) Representative immunohistochemistry for cleaved caspase-3 of pancreatic islets of WT and *Trim27*<sup>-/-</sup> mice (n=3).

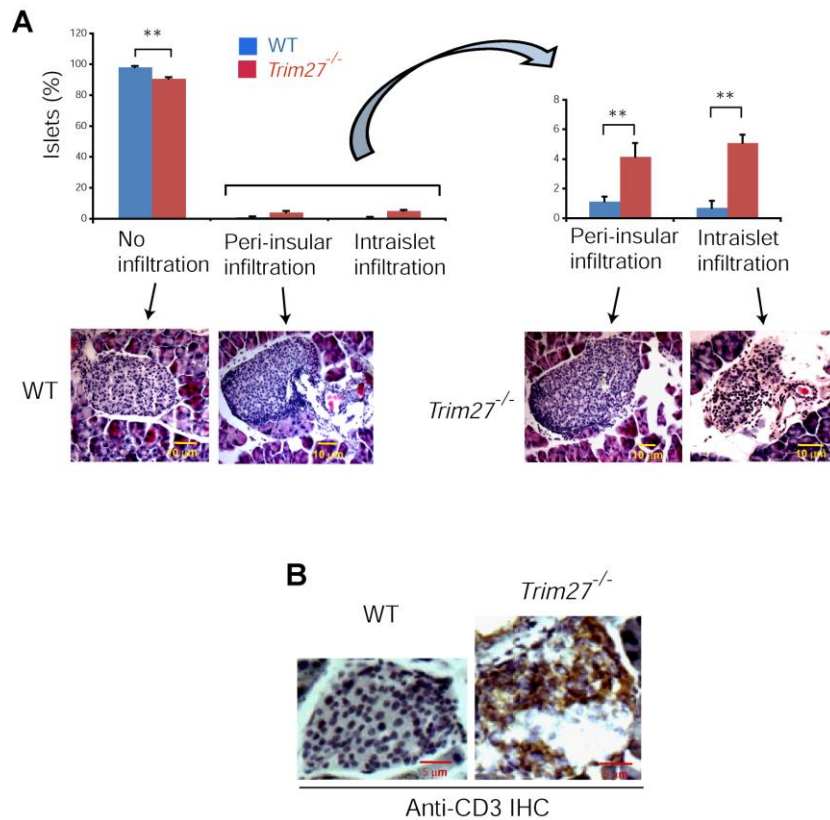


**Figure 4.23 STZ induced diabetic *Trim27*<sup>-/-</sup> mice showed severe infiltration of lymphocytes in pancreatic islet** (A) Histological examination of pancreatic islets. Mice were treated as described in Figure 4.21, and pancreatic sections were stained with hematoxylin and eosin. An average of 75 sections (5  $\mu$ m thickness) from each WT (n = 6) and *Trim27*<sup>-/-</sup> (n = 7) mouse were examined. The degree of infiltration was classified into three types and their frequency was calculated. The average frequency  $\pm$  SEM are shown as a bar graph (upper), and typical sections are shown (below). Scale bar, 10  $\mu$ m (B) Anti-CD3 immunohistochemistry of pancreatic section of STZ treated mice.

## Chapter 5

### 5. Discussion

---

The results of the present study indicate that *Trim27*-deficient mice are resistant to TNF- $\alpha$ /GalN-induced apoptosis, and TRIM27 forms a complex with and polyubiquitinates USP7, which deubiquitinates RIP1 (**Figure 5.1**). There may be multiple forms of ubiquitinated RIP1 which contain a complex structure of Ub in addition to K63-linked Ub. The deubiquitination of various forms of ubiquitinated RIP1 may trigger the formation of complex II, leading to the induction of apoptosis. In the signaling events downstream of complex I, K63-linked polyubiquitination of RIP1 is essential for the activation of NF- $\kappa$ B and thus the induction of cell survival-related genes because this polyubiquitin chain binds to TAB2 and NEMO, activating TAK1 and IKK complexes (**Figure 5.1**) [67, 70-72]. The TRIM27/USP7 complex removed K27-, K29-, and K48-linked poly-Ub chains from RIP1, but had a little effect on K-11- and K-63-linked poly-Ub. Consistent with this, TRIM27 knockdown did not affect the expression of survival-related genes. The addition of K11-linked poly-Ub to RIP1, which binds to NEMO, has been reported [98], but its role in the induction of survival genes is unknown. Although K48-linked ubiquitination is known to target proteins for proteasomal degradation, knockdown of TRIM27 did not increase RIP1 protein levels. These results suggest that RIP1 is modified by complex poly-Ub chains containing K11-, K27-, K29-, K48-, and K63-linked Ub. The Ub structure specificity of TRIM27 differs from that of CYLD and A20, which remove K63-linked poly-Ub chains from RIP1 and suppress the expression of survival-related genes [73-77]. In the absence of

TNF- $\alpha$  treatment, the degree of ubiquitination of RIP1 in *Trim27*<sup>-/-</sup> cells was higher than that in WT cells, and this difference became more dramatic at 30 min and 120 min after TNF- $\alpha$ /CHX treatment (**Figure 4.20**). These results suggest that TRIM27-dependent deubiquitination of RIP1 occurs constitutively in the absence of TNF- $\alpha$ , and its role in the generation of non-ubiquitinated RIP1 becomes more evident in cells exposed to TNF- $\alpha$ , in which the expression of survival genes, including the RIP1 deubiquitinating enzymes A20 and CYLD is suppressed.

TRIM27 ubiquitination of USP7 at Lys-869 is required for USP7-induced deubiquitination of RIP1. The B-box mutant of TRIM27 was able to bind to USP7 but failed to ubiquitinate USP7, whereas the RING finger mutant of TRIM27 ubiquitinated USP7. TRIM family proteins have two types of B-boxes, 1 and 2, and TRIM27 has only B-box 3. The two types of B-box have a similar structure to that of the RING finger [39]. Our results suggest that the B-box functions as a Ub E3 ligase or that the B-box recruits another Ub E3 ligase. The ability of TRIM27 to add K6-, K11-, K27-, K29-, K33-, K48-, and K63-linked poly-Ub to USP7 suggests that the structure of the poly-Ub chains attached to USP7 is complex. USP7 regulates the level of p53 and Mdm2 by inhibiting their degradation via removal of the K48-linked poly-Ub from these proteins [99]. Non-ubiquitinated USP7 actively removes poly-Ub from p53 and Mdm2, indicating that the polyubiquitination of USP7 is not required for its protease activity. Furthermore, non-ubiquitinated USP7 forms a complex with TRIM27, indicating that the polyubiquitination of USP7 is not required for TRIM27/USP7 complex formation. Therefore, the Ub chain on USP7 may function to recruit RIP1 to the TRIM27/USP7

complex. The catalytic site mutant of USP7, but not WT USP7, forms a complex with RIP1 (**Figure 4.14**), suggesting that RIP1 is released immediately after deubiquitination by USP7. Therefore, the attachment of poly-Ub to USP7 may stabilize the transient RIP1/USP7/TRIM27 complex.

TRIM27 and RIP1 were partly localized to mitochondria and peroxisomes. USP7 was also shown to localize to mitochondria [100]. However, as the TRIM27/USP7 complex may have multiple functions, these data do not necessarily indicate that RIP1 deubiquitination occurs in mitochondria. Recently, the peroxisome was shown to function as the signaling platform for antiviral innate immunity [93]; therefore, the TRIM27/USP7 complex could play a role in innate immunity. In fact, TRIM27 was suggested to inhibit the release of human immunodeficiency virus 1 (HIV) and murine leukemia virus (MLV), and to inhibit MLV gene expression [101]. TRIM27 and USP7 were also partly colocalized in the nucleus, suggesting their possible involvement in transcriptional regulation.

It was shown that USP7 binds to TRAF2 and TRAF6 and suppresses the TNF- $\alpha$ -induced NF- $\kappa$ B activation [102]. However, TRIM27 did not affect the TNF- $\alpha$ -dependent NF- $\kappa$ B target gene expression (**Fig. 4.4C**), and TRIM27 did not affect the TRAF6 ubiquitination (data not shown). Furthermore, it is unlikely that all the USP7 proteins form the complex with TRIM27. Therefore, TRIM27 may not interact with TRAF2/6 together with USP7. Overexpression of TRIM27 suppresses IL-1-, virus infection- and TNF- $\alpha$ -induced cytokine production, and TRIM27 has been shown to bind to IKK $\alpha$ /IKK $\beta$  and suppress their activities [60]. However, in the present study,

TRIM27 knockout did not affect the expression of survival-related genes. Overexpression of certain TRIM proteins may result in a specific phenotype that is not induced by loss-of-function. In particular, because the TRIM family of proteins can form hetero-multimers via the coiled-coil region, the overexpression of certain TRIM proteins may affect the function of other members of the family. TRIM21 ubiquitinates TRIM5 and targets it for degradation [103], suggesting that the overexpression of TRIM27 could affect the level of other TRIM protein(s). TRIM27 has also been shown to activate JNK (Jun N-terminal kinase) and induce apoptosis [104], suggesting another possible function that needs to be investigated through loss-of-function assays.

To understand the biological significance of defective apoptosis in *Trim27*<sup>-/-</sup> mice we used the multiple low dose STZ injected mice as a murine model for autoimmune diabetes. STZ is a glucose analog that enters the beta cells through glucose transporter 2 (Glut2) and causes diabetes in mice and rats by selectively destroying pancreatic  $\beta$  cells by DNA alkylation which ultimately initiate the immune reactions against islets mainly by infiltrating T cells and macrophages, which closely resembles human Type I diabetes [105,106]. Moreover, the onset of disease in STZ induced diabetic model is controlled and the animals involved do not have immune abnormalities that complicate studies in models of spontaneous autoimmune diabetes.

Consistent with the well-known concept that defects in apoptosis are frequently associated with autoimmune diseases [107], *Trim27*<sup>-/-</sup> mice were susceptible to STZ-induced diabetes in our study (**Figure 4.21**). Our findings were also consistent with the results of recent genome-wide association studies linking autoimmune diseases

and genetic polymorphisms, which showed an association between human TRIM27 genes and type 1 diabetes [82]. Although in this study we could not show any direct evidence in support of the mechanism of crosstalk between defective apoptosis and autoimmune Type I diabetes but as the *Trim27*<sup>-/-</sup> mice showed increased infiltration of lymphocyte in the pancreas in response to STZ (**Figure 4.23**), we speculate that peripheral lymphocyte homeostasis and self tolerance mechanism to minimize the accumulation of autoreactive lymphocytes might be defective in *Trim27*<sup>-/-</sup> mice due to abrogated TNF- $\alpha$  induced apoptosis. Lymphocyte apoptosis has been reported as a principal system for immune tolerance which is maintained through deletion of self-reactive lymphocytes (by cell death), functional inactivation (anergy), or suppression of cell activation via regulatory lymphocytes [108]. Members of the tumor necrosis factor (TNF) and TNF receptor (TNFR) family play key roles in the development and function of the immune system. Therefore altered regulation of several of these factors, such as TNF, TRAIL, CD40L and FasL, may contribute to a breakdown in immune tolerance and the development of autoimmune disease [108].

Defect in the TNFR family receptors or their downstream signalling pathways have been linked to uncontrolled lymphocyte proliferation in peripheral lymphoid organs, and the development of autoimmune diseases in mice and humans [109-111]. Previously, it has been reported that mutant mice lacking TRAIL (TNF-related apoptosis-inducing ligand) are prone to STZ-induced diabetes [98]. This susceptibility is caused by a defect in the negative selection of thymocytes and the generation of autoreactive T-cells. In addition, TRAF6 deficiency also induces autoimmunity by affecting the development of

thymic stroma cells [112]. Deficiency in mature lymphocyte apoptosis has been also reported to correlate with the development of disease: Studies in *lpr* and *gld* mice, defective in TNFR family protein CD95 and CD95L respectively, confirmed this hypothesis [113]. Moreover, genetic deficiencies of IL-2 or its receptor, crucial elements for T cell susceptibility to antigen-induced apoptosis, lead to lymphoid hyperplasia and autoimmunity. Moreover, it has been demonstrated that patients with autoimmune lymphoproliferative syndromes present mutation in death receptor machinery concerning abnormalities of TNFR family protein CD95/CD95L [111,112]. As TRIM27 is widely expressed in many types of cells, including thymocytes, thymic stroma cells, T-cells, and macrophages, further analysis will be required to elucidate the mechanism by which the loss of TRIM27 affects the development of autoimmune diseases.

Mutation of most of the genes does not result in a disease phenotype, whereas a TRIM27 mutation in one allele could cause disease by expressing a dominant-negative form. TRIM family proteins form multimer complexes through coiled-coil domain interactions. Therefore, the presence of mutant proteins might block the function of WT proteins via formation of a multimer complex, as reported for the p53 tumor suppressor [114]. Further studies with emphasis on the analysis of diabetes patients are necessary to understand the role of TRIM27 in human type 1 diabetes.

A recent study that used *Trim27*-deficient mice, which were independently generated from ours, showed that TRIM27 catalyzes the K48-linked ubiquitination of the class II phosphatidylinositol 3 kinase C2 $\beta$  (PI3KC2 $\beta$ ), promoting inhibition of its enzymatic

activity, and negatively regulates CD4 T-cells by inhibiting TCR-stimulated Ca<sup>2+</sup> influx and cytokine production [63]. TRIM27 also negatively regulates IgE receptor activation and downstream signaling by the same mechanism [64]. Further analyses using *Trim27*<sup>-/-</sup> mice may help to elucidate the uncharacterized physiological roles of TRIM27.

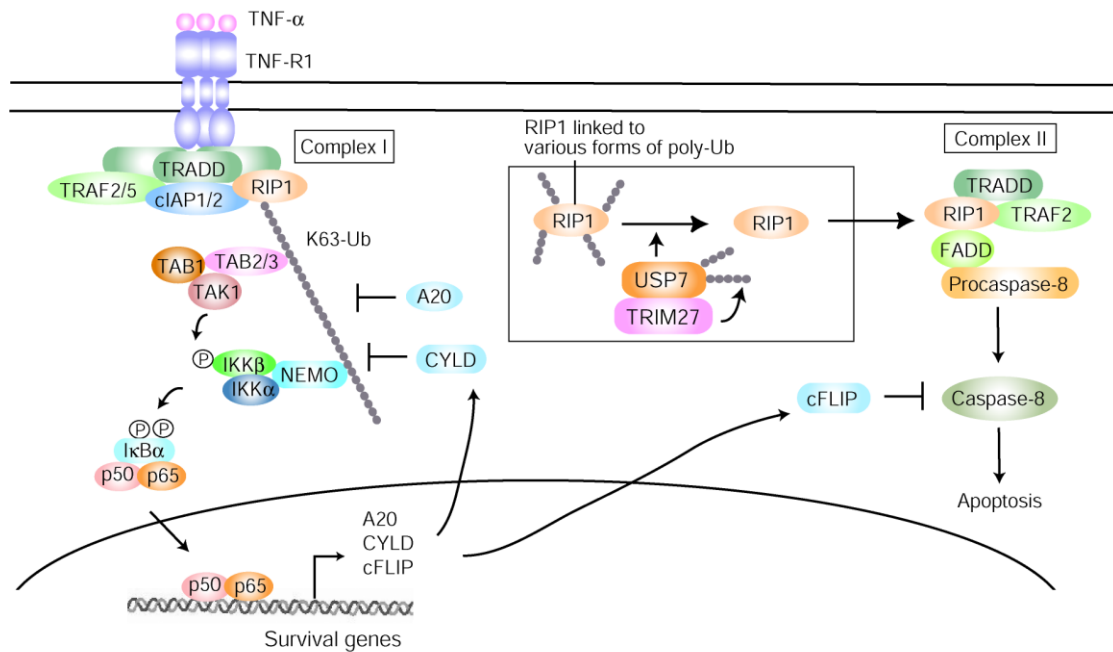


**Figure 5.1 Model describing the role of TRIM27-USP7 in TNF $\alpha$ -induced apoptosis.** Upon binding to TNF $\alpha$ , TNFR1 binds to TRADD and triggers the formation of complex I and II. Complex I, containing TRADD, TRAF2, TRAF5, RIP1, cIAP1 and cIAP2, activates NF- $\kappa$ B. The ubiquitin ligases cIAP1 and cIAP2 catalyze the K-63-linked polyubiquitination of RIP1, which binds to TAB2 and NEMO. This induces activation of TAK1 and IKK complexes, followed by NF- $\kappa$ B activation to induce the transcription of survival genes. Activation of NF- $\kappa$ B triggers the dissociation of RIP1 from complex I and the formation of complex II containing FADD and procaspase-8, which induces apoptosis. Multiple forms of ubiquitinated RIP1, which contains not only K63-linked Ub but also other various forms of Ub, may exist. TRIM27 forms a complex with and ubiquitinates USP7, which deubiquitinates RIP1, upregulating complex II-dependent apoptosis.

## Chapter 6

### 6. Conclusion

---

Tumor necrosis factor  $\alpha$  (TNF- $\alpha$ ) plays a role in apoptosis and proliferation in multiple types of cells, and defects in TNF- $\alpha$ -induced apoptosis are associated with various autoimmune diseases. Here, we show that TRIM27, a tripartite motif (TRIM) protein containing RING finger, B-box, and coiled-coil domains, positively regulates TNF- $\alpha$ -induced apoptosis. *Trim27*-deficient mice are resistant to TNF- $\alpha$ /D-galactosamine-induced hepatocyte apoptosis. *Trim27*-deficient mouse embryonic fibroblasts (MEFs) are also resistant to TNF- $\alpha$ /cycloheximide-induced apoptosis. TRIM27 forms a complex with and ubiquitinates the ubiquitin-specific protease USP7, which deubiquitinates receptor-interacting protein 1 (RIP1), resulting in the positive regulation of TNF- $\alpha$ -induced apoptosis. *Trim27*-deficient mice were susceptible to streptozotocin (STZ)-induced diabetes, a typical autoimmune disease. Our findings indicate that the ubiquitination-deubiquitination cascade mediated by the TRIM27-USP7 complex plays an important role in TNF- $\alpha$ -induced apoptosis.

## Chapter 7

### 7. References

---

1. **Baehrecke, E.H.** 2003. How death shapes life during development. *Nat. Rev. Mol. Cell. Biol.* **3**: 779–787.
2. **Thompson, C.B.** 1995. Apoptosis in the pathogenesis and treatment of disease. *Science* **267**: 1456–1463.
3. **Kerr JF, Wyllie AH, Currie AR.** 1973. Apoptosis: a basic biological phenomenon with wide-ranging implications in tissue kinetics. *Br. J. Cancer.* **26**: 239-257.
4. **Wyllie AH, Kerr JF, Currie AR.** 1980. Cell death: the significance of apoptosis. *Int. Rev. Cytol.* **68**: 251-306.
5. **Cohen JJ, Duke RC.** 1984. Glucocorticoid activation of a calcium-dependent endonuclease in thymocyte nuclei leads to cell death. *J. Immunol.* **132**: 38-43.
6. **Ren Y, Savill J.** 1998. Apoptosis: the importance of being eaten. *Cell Death Differ.* **5**: 563-568.
7. **Kidd VJ, Lahti JM, Teitz T.** 2000. Proteolytic regulation of apoptosis. *Semin. Cell. Dev. Biol.* **11**: 191-201.
8. **Shi Y.** 2003. Mechanisms of caspase activation and inhibition during apoptosis. *Mol. Cell* **9**: 459–470.
9. **Meier P and Vousden KH.** 2007. Lucifer’s labyrinth—ten years of path finding in cell death. *Mol. Cell.* **28**: 746–754.
10. **Green DR and Kroemer G.** 2004. The pathophysiology of mitochondrial cell

death. *Science* **305**: 626–629.

11. **Li P, et al.** 1997. Cytochrome c and dATP-dependent formation of Apaf-1/caspase-9 complex initiates an apoptotic protease cascade. *Cell* **91**:479–489.
12. **de Almagro MC, Vucic D.** 2008. The inhibitor of apoptosis (IAP) proteins are critical regulators of signaling pathways and targets for anti-cancertherapy. *Exp Oncol.* 34:200-211.
13. **Enari M, Sakahira H, Yokoyama H, Okawa K, Iwamatsu A, Nagata SA.** 1998. caspase activated DNase that degrades DNA during apoptosis, and its inhibitor ICAD. *Nature* 391: 43–50.
14. **Glickman MH, Ciechanover A.** 2003. The ubiquitin–proteasome proteolytic pathway: destruction for the sake of construction. *Physiol .Rev.* **82**:373–428.
15. **Hershko A, Ciechanover A.** 1998. The ubiquitin system. *Annu. Rev. Biochem.* **67**:425–479.
16. **Pickart C.** 2000. Ubiquitin in chains. *Trends. Biochem. Sci.* **25**:544–548.
17. **Ikeda F, Dikic I.** 2008. Atypical ubiquitin chains: new molecular signals. ‘Protein Modifications: Beyond the Usual Suspects’ review series. *EMBO Rep.* **9**:536–543.
18. **Kim HT, Kim KP, Lledias F, Kisselev AF, Scaglione KM, Skowyra D, Gygi SP, Goldberg AL.** 2007. Certain pairs of ubiquitin-conjugating enzymes (E2s) and ubiquitin-protein ligases (E3s) synthesize nondegradable forked ubiquitin chains containing all possible isopeptide linkages. *J. Biol. Chem.* **282**:17375–17386.

19. **Varadan R, Assfalg M, Haririnia A, Raasi S, Pickart C, Fushman D.** 2004. Solution conformation of Lys63-linked di-ubiquitin chain provides clues to functional diversity of polyubiquitin signaling. *J. Biol. Chem.* **279**:7055–7064.
20. **Al-Hakim AK, Zagorska A, Chapman L, Deak M, Peggie M, Alessi DR.** 2008. Control of AMPK-related kinases by USP9X and atypical Lys(29)/Lys(33)-linked polyubiquitin chains. *Biochem. J.* **411**:249–260.
21. **Bernassola F, Karin M, Ciechanover A, Melino G.** 2008. The HECT family of E3 ubiquitin ligases: multiple players in cancer development. *Cancer. Cell.* **14**:10–21.
22. **Chastagner P, Israel A, Brou C.** 2006. Itch/AIP4 mediates Deltex degradation through the formation of K29-linked polyubiquitin chains. *EMBO Rep.* **7**:1147–1154.
23. **Wang M, Cheng D, Peng J, Pickart CM.** 2006. Molecular determinants of polyubiquitin linkage selection by an HECT ubiquitin ligase. *EMBO J.* **25**:1710–1719.
24. **Spence J, Sadis S, Haas AL, Finley D.** 1995. A ubiquitin mutant with specific defects in DNA repair and multiubiquitination. *Mol. Cell. Biol.* **15**:1265–1274.
25. **Wu CJ, Conze DB, Li T, Srinivasula SM, Ashwell JD.** 2006. Sensing of Lys 63-linked polyubiquitination by NEMO is a key event in NF-kappaB activation. *Nat. Cell. Biol.* **8**:398–406.
26. **Mukhopadhyay D, Riezman H.** 2007. Proteasome-independent functions of ubiquitin in endocytosis and signaling. *Science* **315**:201–205.

27. **Arnason T, Ellison MJ.** 1994. Stress resistance in *Saccharomyces cerevisiae* is strongly correlated with assembly of a novel type of multiubiquitin chain. *Mol. Cell. Biol.* **14**:7876–7884.
28. **Konstantinova IM, Tsimokha AS, Mittenberg AG.** 2008. Role of proteasomes in cellular regulation. *Int. Rev. Cell. Mol. Biol.* **267**:59–124.
29. **Reyes-Turcu FE, Ventii KH, Wilkinson KD.** 2009. Regulation and cellular roles of ubiquitin-specific deubiquitinating enzymes. *Annu. Rev. Biochem.* **78**:363–397.
30. **Sorokin AV, Kim ER, Ovchinnikov LP.** 2009. Proteasome system of protein degradation and processing. *Biochemistry* **74**:1411–1443.
31. **Lee JC, Peter ME.** 2003. Regulation of apoptosis by ubiquitination. *Immunol. Rev.* **193**:39-47.
32. **Schwartz LM, Myer A, Kosz L, Engelstein M, Maier C.** 1990. Activation of polyubiquitin gene expression during developmentally programmed cell death. *Neuron* **5**: 411–419.
33. **Delic J, Morange M, Magdelenat H.** 1994. Ubiquitin pathway involvement in human lymphocyte gamma-irradiation induced apoptosis. *Mol. Cell. Biol.* **13**: 4875–4884.
34. **Jang, M. et al.** 2007. Caspase-7 mediated cleavage of proteasome subunits during apoptosis. *Biochem. Biophys. Res. Commun.* **363**: 388–394.
35. **Sun, X.M. et al.** 2004. Caspase activation inhibits proteasome function during apoptosis. *Mol. Cell.* **14**: 81–94.

36. **Ramakrishna S, Suresh B, Baek KH.** 2011. The role of deubiquitinating enzymes in apoptosis. *Cell. Mol. Life Sci.* **68**:15-26.
37. **Meroni G, Diez-Roux G.** 2005. TRIM/RBCC, a novel class of 'single protein RING finger' E3 ubiquitin ligases. *Bioessays* **27**:1147–1157.
38. **Joazeiro CA, Weissman AM.** 2000. RING finger proteins: mediators of ubiquitin ligase activity. *Cell* **102**:549-553.
39. **Massiah MA, Simmons BN, Short KM, Cox TC.** 2006. Solution structure of the RBCC/TRIM B-box1 domain of human MID1: B-box with a RING. *J. Mol. Biol.* **358**:532-545.
40. **Reymond A, Meroni G, Fantozzi A, Merla G, Cairo S, Luzi L, Riganelli D, Zanaria E, Messali S, Cainarca S, Guffanti A, Minucci S, Pelicci PG, Ballabio A.** 2001. The tripartite motif family identifies cell compartments. *EMBO J.* **20**:2140-2151.
41. **Freemont PS.** 1994. The RING finger. A novel protein sequence motif related to the zinc finger. *Ann. NY. Acad. Sci.* **684**: 174 –193.
42. **Barlow PN, Luisi B, Milner A, Elliott M, Everett R.** 1994. Structure of the C3HC4 domain by 1H-nuclear magnetic resonance spectroscopy. A new structural class of zinc-finger. *J. Mol. Biol.* **237**:201–211.
43. **Borden KL, Boddy MN, Lally J, O'Reilly NJ, Martin S, et al.** 1995. The solution structure of the RING finger domain from the acute promyelocytic leukaemia proto-oncoprotein PML. *EMBO J.* **14**:1532–1541.
44. **Freemont PS.** 2000. RING for destruction? *Curr. Biol.* **10**: R84–87.

45. **Torok M, Etkin LD.** 2001. Two B or not two B? Overview of the rapidly expanding B-box family of proteins. *Differentiation* **67**:63–71.
46. **Reymond A, Meroni G, Fantozzi A, Merla G, Cairo S, et al.** 2001. The tripartite motif family identifies cell compartments. *EMBO J.* **20**:2140–2151.
47. **Joazeiro CA, Weissman AM.** 2000. RING finger proteins: mediators of ubiquitin ligase activity. *Cell* **102**:549–553.
48. **Borden KL, Martin SR, O'Reilly NJ, Lally JM, Reddy BA, et al.** 1994. Characterisation of a novel cysteine/histidine-rich metal binding domain from *Xenopus* nuclear factor XNF7. *FEBS Lett.* **335**:255–260.
49. **Henry J, Mather IH, McDermott MF, Pontarotti P.** 1998. B30.2-like domain proteins: update and new insights into a rapidly expanding family of proteins. *Mol. Biol. Evol.* **15**:1696–1705.
50. **Slack FJ, Ruvkun G.** 1998. A novel repeat domain that is often associated with RING finger and B- box motifs. *Trends. Biochem. Sci.* **23**:474–475.
51. **Ozato K, Shin DM, Chang TH, Morse HCIII.** 2008. TRIM family proteins and their emerging roles in innate immunity. *Nat. Rev. Immunol.* **8**:849-860.
52. **Gack MU, Shin YC, Joo CH, Urano T, Liang C, Sun L, Takeuchi O, Akira S, Chen Z, Inoue S, Jung JU.** 2007. TRIM25 RING-finger E3 ubiquitin ligase is essential for RIG-I-mediated antiviral activity. *Nature* **446**:916-920.
53. **Shi M, Deng W, Bi E, Mao K, Ji Y, Lin G, Wu X, Tao Z, Li Z, Cai X, Sun S, Xiang C, Sun B.** 2008. TRIM30 $\alpha$  negatively regulates TLR-mediated NF- $\kappa$ B activation by targeting TAB2 and TAB3 for degradation. *Nat. Immunol.*

9:369-377.

54. **Tsuchida T, Zou J, Saitoh T, Kumar H, Abe T, Matsuura Y, Kawai T, Akira S.** 2010. The ubiquitin ligase TRIM56 regulates innate immune responses to intracellular double-stranded DNA. *Immunity* **33**:765-776.
55. **Arimoto K, Funami K, Saeki Y, Tanaka K, Okawa K, Takeuchi O, Akira S, Murakami Y, Shimotohno K.** 2010. Polyubiquitin conjugation to NEMO by tripartite motif protein 23 (TRIM23) is critical in antiviral defense. *Proc. Natl. Acad. Sci. USA* **107**:15856-15861.
56. **Takahashi M, Ritz J, Cooper GM.** 1985. Activation of a novel human transforming gene, *ret*, by DNA rearrangement. *Cell* **42**:581–588.
57. **Shimono Y, Murakami H, Kawai K, Wade PA, Shimokata K, Takahashi M.** 2004. Mi-2 $\beta$  associates with BRG1 and RET finger protein at the distinct regions with transcriptional activating and repressing abilities. *J. Biol. Chem.* **278**:51638–51645.
58. **Krützfeldt M, Ellis M, Weekes DB, Bull JJ, Eilers M, Vivanco MD, Sellers WR, Mittnacht S.** 2005. Selective ablation of retinoblastoma protein function by the RET finger protein. *Mol. Cell* **18**:213-224.
59. **Harbers M, Nomura T, Ohno S, Ishii S.** 2001. Intracellular localization of the Ret finger protein depends on a functional nuclear export signal and protein kinase C activation. *J. Biol. Chem.* **276**:48596-48607.
60. **Zha J, Han KJ, Xu LG, He W, Zhou Q, Chen D, Zhai Z, Shu HB.** 2006. The Ret finger protein inhibits signaling mediated by the noncanonical and canonical

- I $\kappa$ B kinase family members. *J. Immunol.* **176**:1072-1080.
61. **Dho SH, Kwon KS.** 2004. The Ret finger protein induces apoptosis via its RING finger-B box-coiled-coil motif. *J. Biol. Chem.* **278**:31902-31908.
  62. **Kee HJ, Kim JR, Joung H, Choe N, Lee SE, Eom GH, Kim JC, Geyer SH, Jijiwa M, Kato T, Kawai K, Weninger WJ, Seo SB, Nam KI, Jeong MH, Takahashi M, Kook H.** 2013. Ret finger protein inhibits muscle differentiation by modulating serum response factor and enhancer of polycomb1. *Cell Death Differ.* **19**:121-131.
  63. **Cai X, Srivastava S, Sun Y, Li Z, Wu H, Zuvella-Jelaska L, Li J, Salamon RS, Backer JM, Skolnik EY.** 2011. Tripartite motif containing protein 27 negatively regulates CD4 T cells by ubiquitinating and inhibiting the class II PI3K-C2 $\beta$ . *Proc. Natl. Acad. Sci. USA* **108**:20072-20077.
  64. **Srivastava S, Cai X, Li Z, Sun Y, Skolnik EY.** 2013. Phosphatidylinositol-3-kinase C2 $\beta$  and TRIM27 function to positively and negatively regulate IgE receptor activation of mast cells. *Mol. Cell. Biol.* **32**:3132-3139.
  65. **Chen G, Goeddel DV.** 2003. TNF-R1 signaling: a beautiful pathway. *Science* **296**:1634-1635.
  66. **Croft M.** 2009. The role of TNF superfamily members in T-cell function and diseases. *Nat. Rev. Immunol.* **9**:271-285.
  67. **Vucic D, Dixit VM, Wertz IE.** 2011. Ubiquitylation in apoptosis: a post-translational modification at the edge of life and death. *Nat. Rev. Mol. Cell.*

Biol. **12**:439-453.

68. **Aggarwal BB.** 2003. Signalling pathways of the TNF superfamily: a double-edged sword. *Nat. Rev. Immunol.* **3**:745-156.
69. **Micheau O, Tschopp J.** 2004. Induction of TNF receptor I-mediated apoptosis via two sequential signaling complexes. *Cell* **114**:181-190.
70. **Mahoney DJ, Cheung HH, Mrad RL, Plenchette S, Simard C, Enwere E, Arora V, Mak TW, Lacasse EC, Waring J, Korneluk RG.** 2008. Both cIAP1 and cIAP2 regulate TNF $\alpha$ -mediated NF- $\kappa$ B activation. *Proc. Natl. Acad. Sci. USA* **105**:11778-11784.
71. **Bertrand MJ, Milutinovic S, Dickson KM, Ho WC, Boudreault A, Durkin J, Gillard JW, Jaquith JB, Morris SJ, Barker PA.** 2008. cIAP1 and cIAP2 facilitate cancer cell survival by functioning as E3 ligases that promote RIP1 ubiquitination. *Mol. Cell* **30**:689-700.
72. **Ea CK, Deng L, Xia ZP, Pineda G, Chen ZJ.** 2006. Activation of IKK by TNF- $\alpha$  requires site-specific ubiquitination of RIP1 and polyubiquitin binding by NEMO. *Mol. Cell* **22**:245-257.
73. **Wertz IE, O'Rourke KM, Zhou H, Eby M, Aravind L, Seshagiri S, Wu P, Wiesmann C, Baker R, Boone DL, Ma A, Koonin EV, Dixit VM.** 2004. De-ubiquitination and ubiquitin ligase domains of A20 downregulate NF- $\kappa$ B signalling. *Nature* **430**:694-699.
74. **Shembade N, Ma A, Harhaj EW.** 2010. Inhibition of NF- $\kappa$ B signaling by A20 through disruption of ubiquitin enzyme complexes. *Science* **327**:1135-1139.

75. **Trompouki E, Hatzivassiliou E, Tsihritzis T, Farmer H, Ashworth A, Mosialos G.** 2004. CYLD is a deubiquitinating enzyme that negatively regulates NF- $\kappa$ B activation by TNFR family members. *Nature* **424**:793-796.
76. **Brummelkamp TR, Nijman SM, Dirac AM, Bernards R.** 2004. Loss of the cylindromatosis tumour suppressor inhibits apoptosis by activating NF- $\kappa$ B. *Nature* **424**:797-801.
77. **Long JS, Ryan KM.** 2012. New frontiers in promoting tumour cell death: targeting apoptosis, necroptosis and autophagy. *Oncogene* **31**:5045-560.
78. **Eguchi K.** 2001. Apoptosis in autoimmune diseases. *Internal Medicine* **40**: 275-284
79. **Mackay F and Kalled SL.** 2003. TNF ligands and receptors in autoimmunity: an update. *Curr. Opin. Immunol.* **14**:783–790
80. **Kollias G, Kontoyiannis D.** 2003. Role of TNF/TNFR in autoimmunity: specific TNF receptor blockade may be advantageous to anti-TNF treatments. *Cytokine & Growth Factor Reviews* **13**: 315–321
81. **Jefferies C, Wynne C, Higgs R.** 2011. Antiviral TRIMs: friend or foe in autoimmune and autoinflammatory disease? *Nat .Rev. Immunol.* **11**:617-625
82. **Baranzini SE.** 2009. The genetics of autoimmune diseases: a networked perspective. *Curr. Opin. Immunol.* **21**:596-605
83. **Barcellos LF, May SL, Ramsay PP, Quach HL, Lane JA, Nititham J, Noble JA, Taylor KE, Quach DL, Chung SA, Kelly JA, Moser KL, Behrens TW, Seldin MF, Thomson G, Harley JB, Gaffney PM, Criswell LA.** 2009.

High-density SNP screening of the major histocompatibility complex in systemic lupus erythematosus demonstrates strong evidence for independent susceptibility regions. *PLoS Genet.* **5**:e1000696.

84. **Takagi T, Harada J, Ishii S.** 2001. Murine Schnurri-2 is required for positive selection of thymocytes. *Nat. Immunol.* **2**:1048-1054.
85. **Bellenger J, Bellenger S, Bataille A, Massey KA, Nicolaou A, Rialland M, Tessier C, Kang JX, Narce M.** 2011. High pancreatic n-3 fatty acids prevent STZ-induced diabetes in fat-1 mice: inflammatory pathway inhibition. *Diabetes* **60**:1090-1099.
86. **Thapa RJ, Basagoudanavar S, Nogusa S, Irrinki K, Mallilankaraman K, Slifker MJ, Beg AA, Madesh M, Balachandran S.** 2011. NF- $\kappa$ B protects cells from interferon- $\gamma$ -induced RIP1-dependent necroptosis. *Mol. Cell. Biol.* **31**: 2934-2946.
87. **Khan MM, Nomura T, Kim H, Kaul SC, Wadhwa R, Zhong S, Pandolfi PP, Ishii S.** 2004. The fusion oncoprotein PML-RAR $\alpha$  induces endoplasmic reticulum (ER)-associated degradation of N-CoR and ER stress. *J. Biol. Chem.* **279**:11814-11824.
88. **Yamauchi T, Ishidao T, Nomura T, Shinagawa T, Tanaka Y, Yonemura S, Ishii S.** 2008. A B-Myb complex containing clathrin and filamin is required for mitotic spindle function. *EMBO J.* **27**:1852-1863.
89. **Ramakrishnan P, Baltimore D.** 2011. Sam68 is required for both NF- $\kappa$ B activation and apoptosis signaling by the TNF receptor. *Mol. Cell.* **43**: 167-179

90. **Canning M, Boutell C, Parkinson J, Everett RD.** 2004. A RING finger ubiquitin ligase is protected from autocatalyzed ubiquitination and degradation by binding to ubiquitin-specific protease USP7. *J. Biol. Chem.* **279**:38160-38168.
91. **Lehmann V, Freudenberg MA, Galanos C.** 1987. Lethal toxicity of lipopolysaccharide and tumor necrosis factor in normal and D-galactosamine-treated mice. *J. Exp. Med.* **165**:657-664.
92. **Temkin V, Huang Q, Liu H, Osada H, Pope RM.** 2006. Inhibition of ADP/ATP exchange in receptor-interacting protein-mediated necrosis. *Mol. Cell. Biol.* **26**:2215-2225.
93. **Dixit E, Boulant S, Zhang Y, Lee AS, Odendall C, Shum B, Hacohen N, Chen ZJ, Whelan SP, Fransen M, Nibert ML, Superti-Furga G, Kagan JC.** 2010. Peroxisomes are signaling platforms for antiviral innate immunity. *Cell* **141**:668-681.
94. **Hu M, Li P, Li M, Li W, Yao T, Wu JW, Gu W, Cohen RE, Shi Y.** 2003. Crystal structure of a UBP-family deubiquitinating enzyme in isolation and in complex with ubiquitin aldehyde. *Cell* **111**:1041-1054.
95. **Fernández-Montalván A, Bouwmeester T, Joberty G, Mader R, Mahnke M, Pierrat B, Schlaeppli JM, Worpenberg S, Gerhartz B.** 2007. Biochemical characterization of USP7 reveals post-translational modification sites and structural requirements for substrate processing and subcellular localization. *FEBS J.* **274**:4256-4270.
96. **Colland F, Formstecher E, Jacq X, Reverdy C, Planquette C, Conrath S,**

- Trouplin V, Bianchi J, Aushev VN, Camonis J, Calabrese A, Borg-Capra C, Sippl W, Collura V, Boissy G, Rain JC, Guedat P, Delansorne R, Daviet L.** 2009. Small-molecule inhibitor of USP7/HAUSP ubiquitin protease stabilizes and activates p53 in cells. *Mol. Cancer Ther.* **8**:2286-2295.
97. **Lamhamedi-Cherradi, S.E., Zheng, S.J., Maguschak, K.A., Peschon, J. & Chen, Y.H.** 2004. Defective thymocyte apoptosis and accelerated autoimmune diseases in *TRAIL*<sup>-/-</sup> mice. *Nat. Immunol.* **4**:255-260.
98. **Dynek JN, Goncharov T, Dueber EC, Fedorova AV, Izrael-Tomasevic A, Phu L, Helgason E, Fairbrother WJ, Deshayes K, Kirkpatrick DS, Vucic D.** 2010. c-IAP1 and UbcH5 promote K11-linked polyubiquitination of RIP1 in TNF signalling. *EMBO J.* **29**:4198-4209.
99. **Li M, Brooks CL, Kon N, Gu W.** 2004. A dynamic role of HAUSP in the p53-Mdm2 pathway. *Mol. Cell.* **13**:879-886.
100. **Marchenko ND, Wolff S, Erster S, Becker K, Moll UM.** 2007. Monoubiquitylation promotes mitochondrial p53 translocation. *EMBO J.* **26**:923-934.
101. **Uchil PD, Quinlan BD, Chan WT, Luna JM, Mothes W.** 2008. TRIM E3 ligases interfere with early and late stages of the retroviral life cycle. *PLoS Pathog.* **4**:e16.
102. **Zapata JM, Pawlowski K, Haas E, Ware CF, Godzik A, Reed JC.** 2001. A diverse family of proteins containing tumor necrosis factor receptor-associated factor domains. *J. Biol. Chem.* **276**:24242-24253.

103. **Yamauchi K, Wada K, Tanji K, Tanaka M, Kamitani T.** 2008. Ubiquitination of E3 ubiquitin ligase TRIM5 alpha and its potential role. *FEBS J.* **275**:1540–1555.
104. **Dho SH, Kwon KS.** 2004. The Ret finger protein induces apoptosis via its RING finger-B box-coiled-coil motif. *J. Biol. Chem.* **278**:31902-31908.
105. **Elsner M, Guldbakke B, Tiedge M, Munday R, Lenzen S.** 2000. Relative importance of transport and alkylation for pancreatic beta-cell toxicity of streptozotocin. *Diabetologia* **43**:1528-1534.
106. **Like AA, Rossini AA.** 1976. Streptozotocin-induced pancreatic insulinitis: new model of diabetes mellitus. *Science* **193**:415-417.
107. **Cacciapaglia F, Spadaccio C, Chello M, Gigante A, Coccia R, Afeltra A, Amorso A.** 2009. Apoptotic molecular mechanisms implicated in autoimmune diseases. *Eur. Rev. Med. Pharmacol. Sci.* **13**:23-40.
108. **Mackay F, Kalled SL.** 2003. TNF ligands and receptors in autoimmunity: an update. *Curr. Opin. Immunol.* **14**:783-790.
109. **Koetz K, Bryl E, Spickschen K, O'fallon WM, Goronzy JJ, Weyand CM.** 2000. T cell homeostasis in patients with rheumatoid arthritis. *Proc. Natl. Acad. Sci. USA* **97**: 9203-9208.
110. **Wang J, Lenardo MJ.** 1997. Molecules involved in cell death and peripheral tolerance. *Curr. Opin. Immunol.* **9**: 818-825.
111. **Sneller MC, Wang J, Dale JK, Strober W, Middleton LA, Choi Y, Fleisher TA, Lim MS, Jaffe ES, Puck JM, Lenardo MJ, Straus SE.** 1997. Clinical,

- immunologic, and genetic features of an autoimmune lymphoproliferative syndrome associated with abnormal lymphocyte apoptosis. *Blood* **89**: 1341-1348.
112. **Akiyama, T. *et al.*** 2005. Dependence of self-tolerance on TRAF6-directed development of thymic stroma. *Science* **308**: 248-251.
113. **Chen C, LiH, Tian Q, Beardall M, Xu Y, Casanova N, Weigert M.** 2006. Selection of anti-double-stranded DNA B cells in autoimmune MRL-*lpr/lpr* mice. *J. Immunol.* **176**: 5183-5190.
114. **Brachmann, R.K., Vidal, M. & Boeke, J.D.** 1996. Dominant-negative p53 mutations selected in yeast hit cancer hot spots. *Proc. Natl. Acad. Sci. USA* **93**: 4091-4095.

## 参 考 論 文

## 参 考 論 文 reference journal

1. Zaman MM, Nomura T, Takagi T, Okamura T, Jin W, Shinagawa T, Tanaka Y, Ishii S. Ubiquitination-deubiquitination by the TRIM27-USP7 Complex Regulates TNF- $\alpha$ -induced Apoptosis. *Mol Cell Biol.*, 2013, 33(24):4971-4984.
2. Zaman MM, Shinagawa T, Ishii S. *Trim27*-deficient mice are susceptible to streptozotocin-induced diabetes. *FEBS Open Bio.*, 2013, 4:60-64.

参考論文については学術雑誌掲載論文から構成されていますが、著作権者(出版社、学会等)の許諾を得ていないため、筑波大学では電子化・公開しておりません。

なお、下記については電子ジャーナルとして出版社から公開されています。契約している場合は全文を読むことができます。詳しくは下記のリンク先をご覧ください。

論文 1) <http://mcb.asm.org/content/33/24/4971>

論文 2) <http://dx.doi.org/10.1016/j.fob.2013.12.002>